第6回特定・宇宙ニュートリノ研究会
2001年6月2日

Solar neutrino results from Super-Kamiokande

M.Nakahata
ICRR, Univ. of Tokyo

- Introduction
- Detection principle
- SK detector performance
- Detector calibration
- Analysis
- Flux, day/night, spectrum
- Neutrino oscillations
- Future work
- Conclusion

Oscillation parameters based on flux of Homestake, GALLEX, SAGE and SK

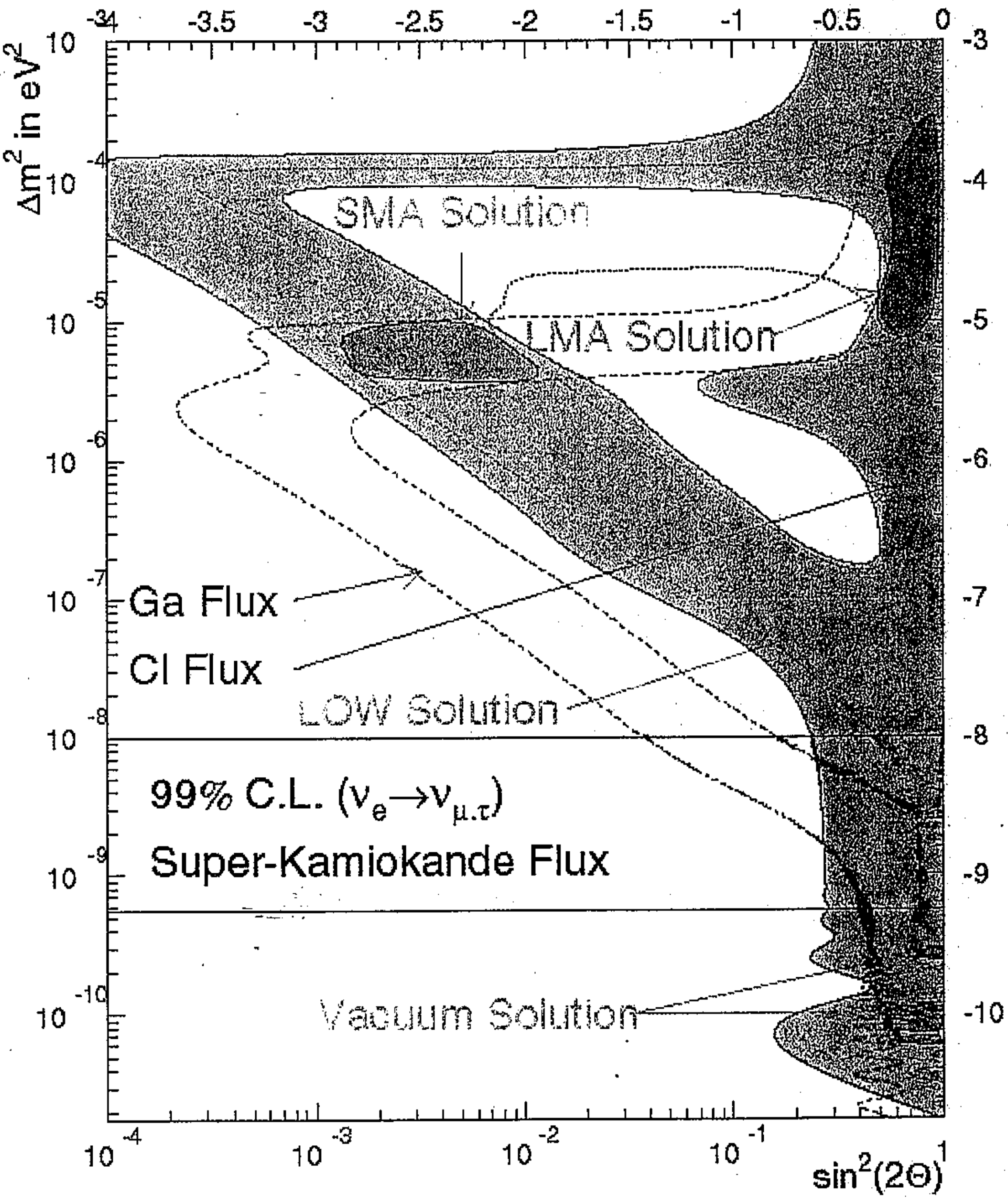

Super-Kamiokade detector

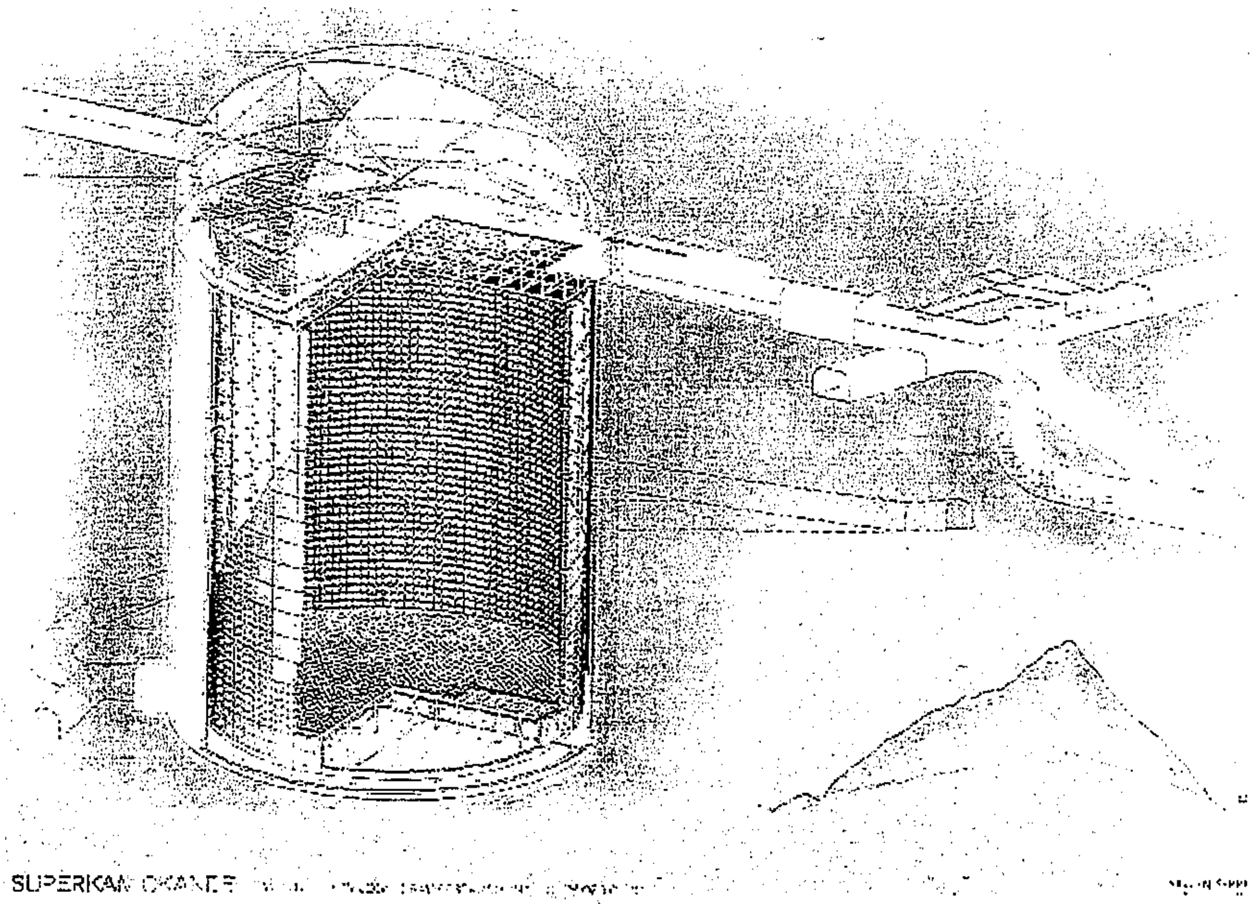

50,000 ton water Cherenkov detector
(22.5 kton fiducial volume)

1000m underground (2700 m.w.e.)

11,146 20-inch PMTs for inner detector

1,885 8-inch PMTs for outer detector

Typical low energy event

- Timing information → vertex position
- Ring pattern → Direction
- # of hit PMTs → Energy

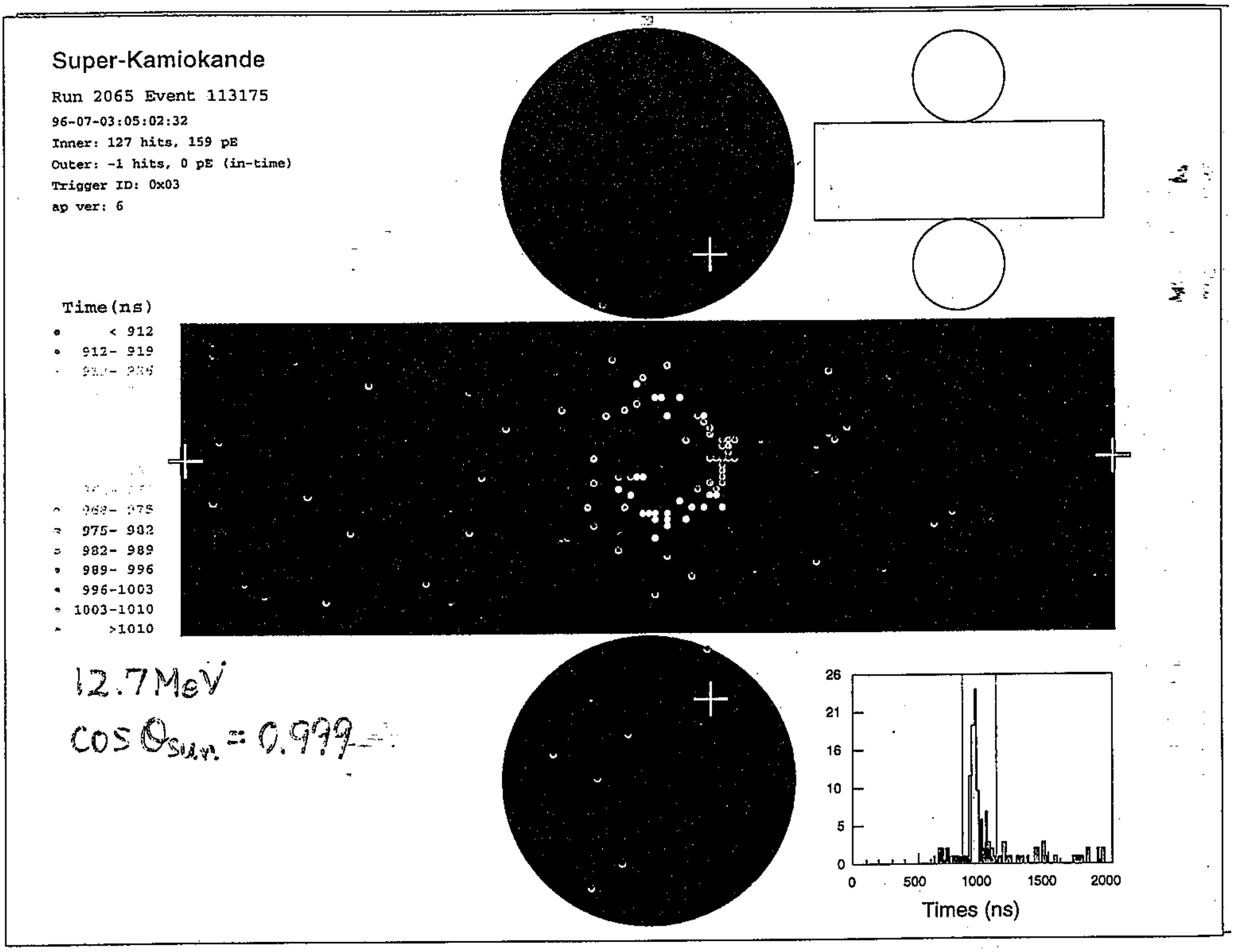

Detect solar neutrinos by

$\nu + e^- \rightarrow \nu + e^-$ scattering

νe scattering kinematics

νe → νe scattering

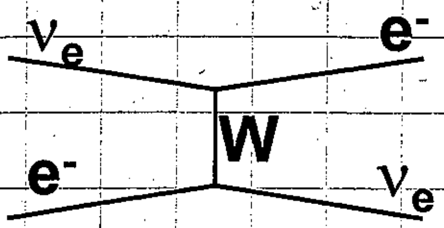

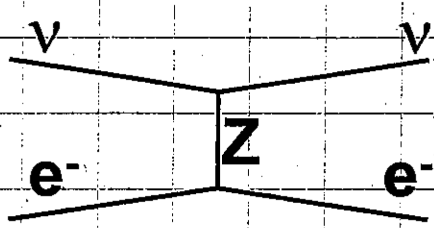

$$\frac{d\sigma}{dT} = \frac{2G_F^2 m_e}{\pi}\left[g_L^2 + g_R^2(1-T/E_\nu)^2 - g_L g_R m_e T/E_\nu^2\right]$$

T: kinetic energy of recoil electron
$g_L = (\pm 1/2 + \sin^2\theta_W)$ for ν_e and $\nu_{\mu(\tau)}$
$g_R = \sin^2\theta_W$

e.g. $d\sigma/dT$ for 10 MeV neutrino

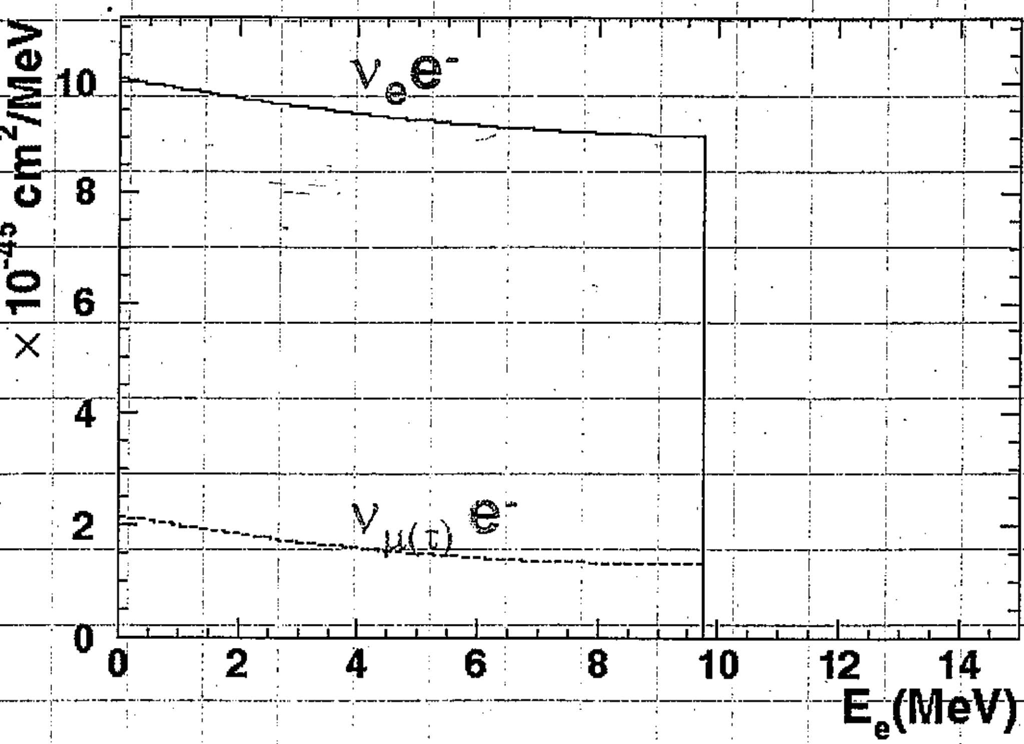

νe scattering kinematics

^{8}B solar neutrino spectrum

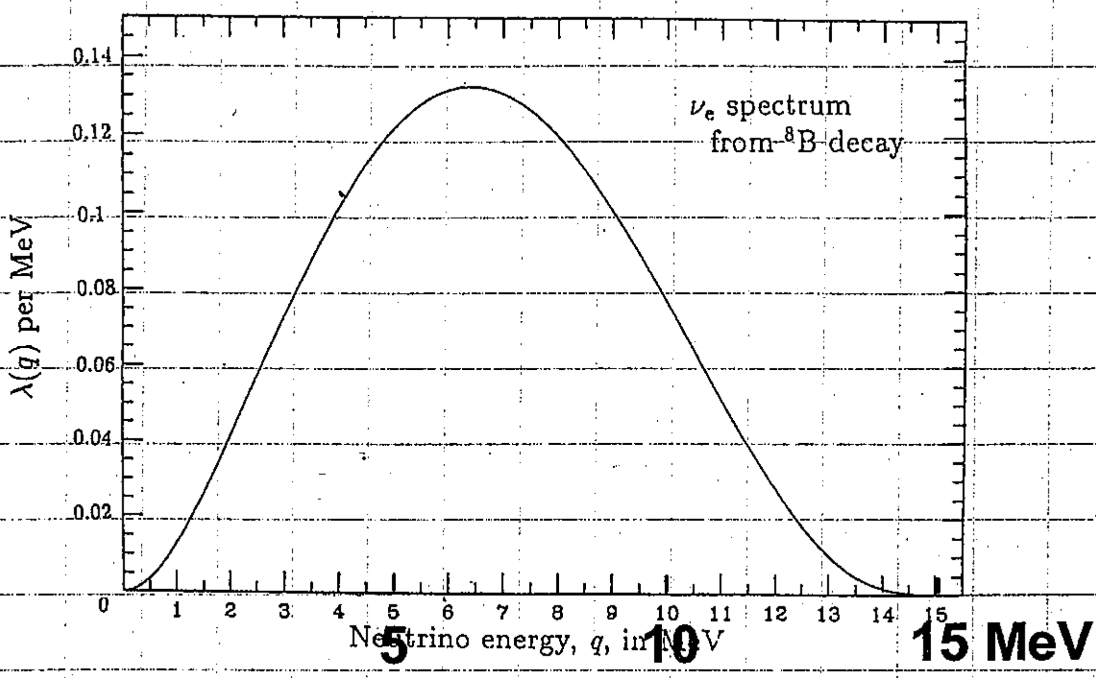

Total cross section for ^{8}B neutrinos

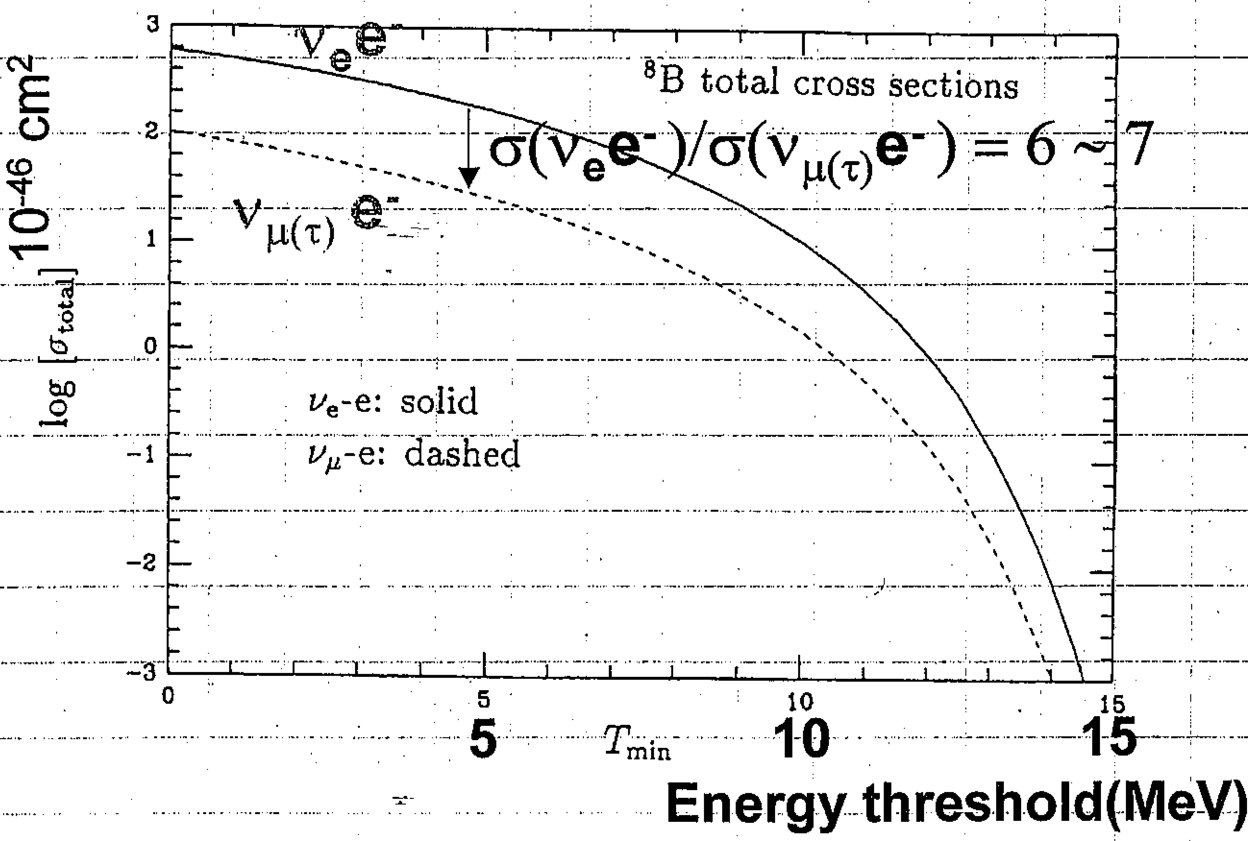

Fraction of ν_e induced events in ν+e scattering

$$R(\nu_e) = \frac{\#\text{ of } \nu_e e^- \text{ induced events}}{\#\text{ of } (\nu_e e^- + \nu_{\mu(\tau)} e^-) \text{ induced events}}$$

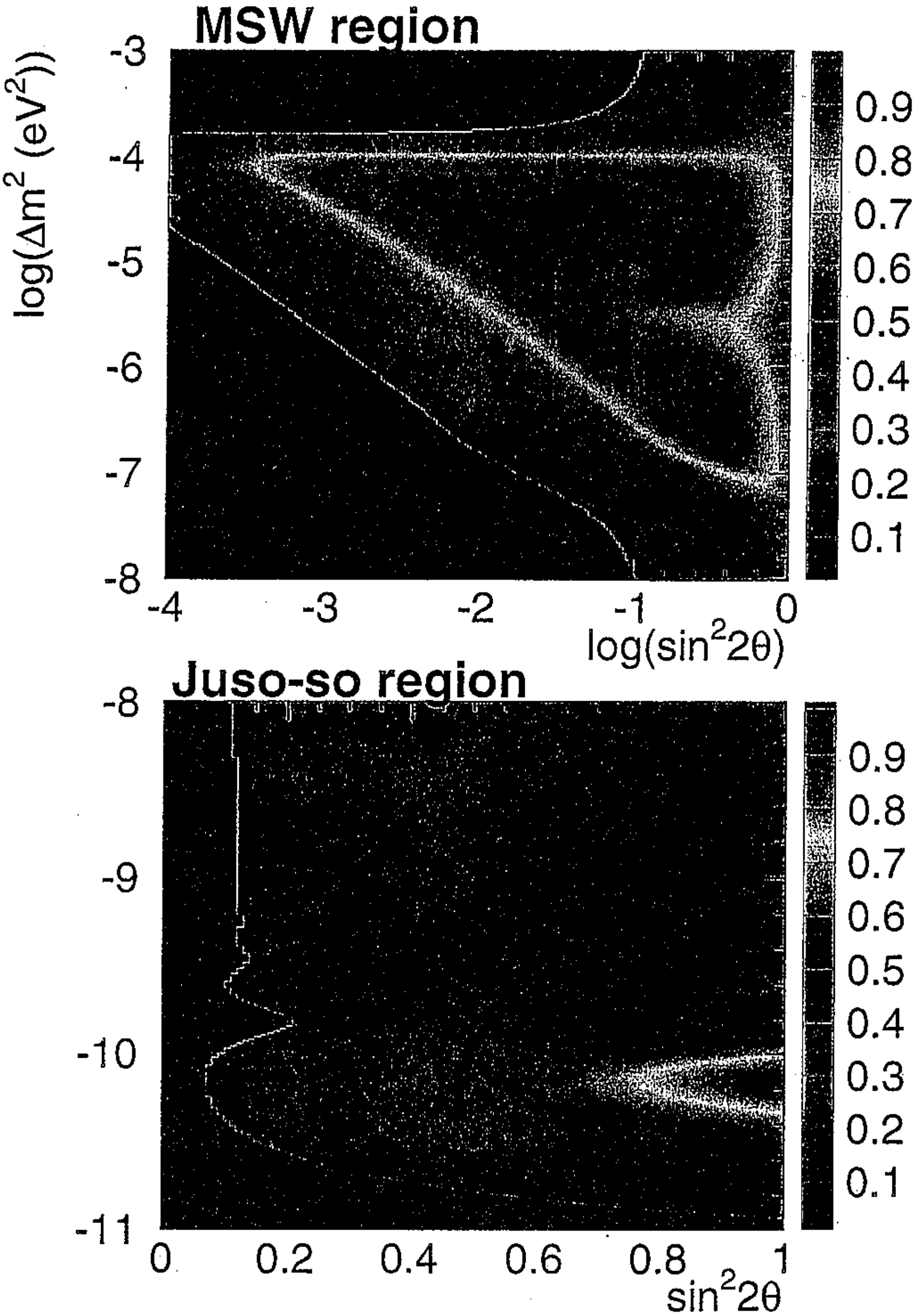

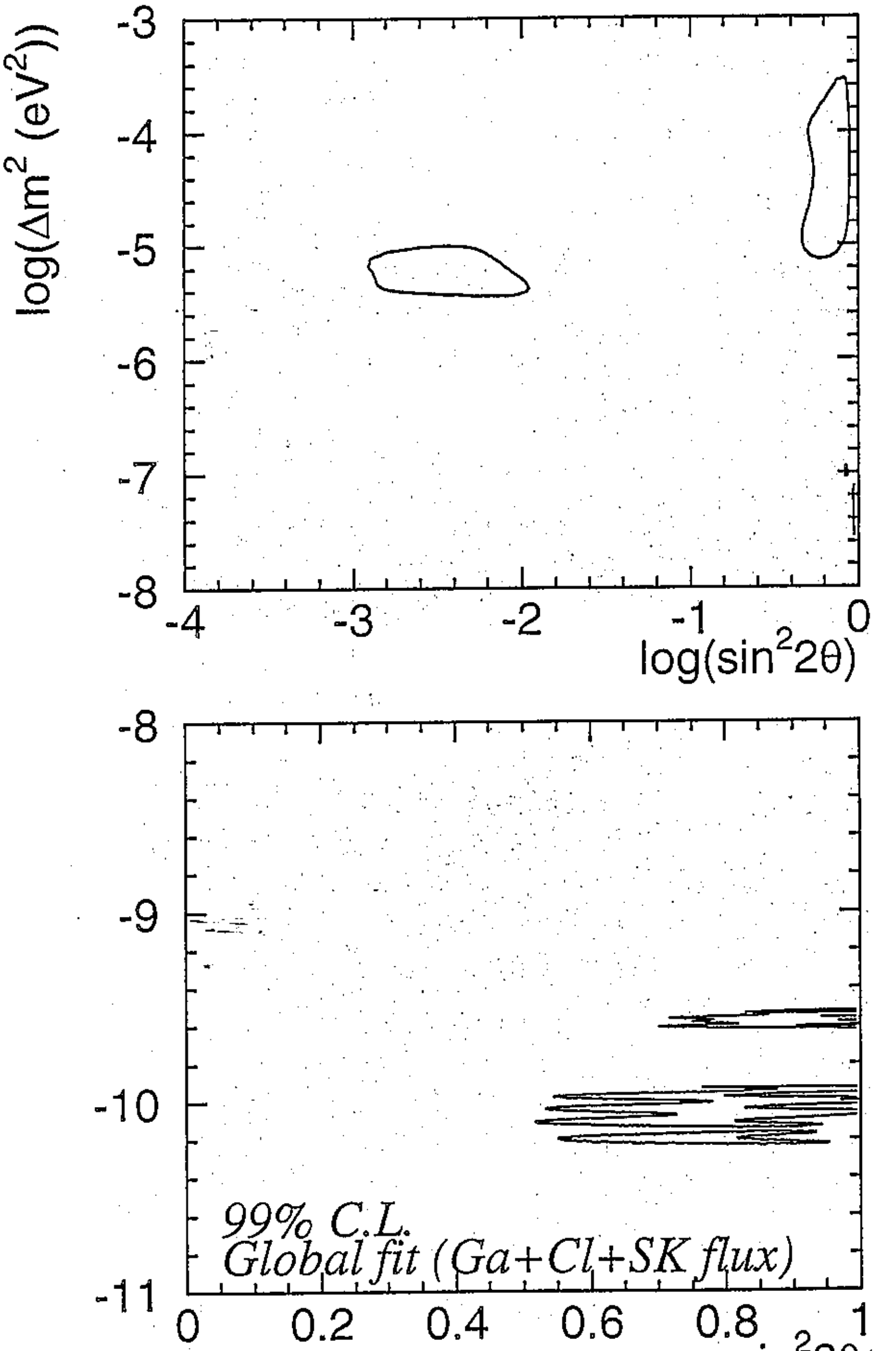
log(Δm² (eV²))
-3
-4
-5
-6
-7
-8
-4
-3
-2
-1
0
log(sin²2θ)
-8
-9
-10
-11
0
0.2
0.4
0.6
0.8
1
sin²2θ
99% C.L.
Global fit (Ga+Cl+SK flux)

LINAC calibration

Precise calibration of absolute energy scale, energy resolution, and angular resolution using electron LINAC.

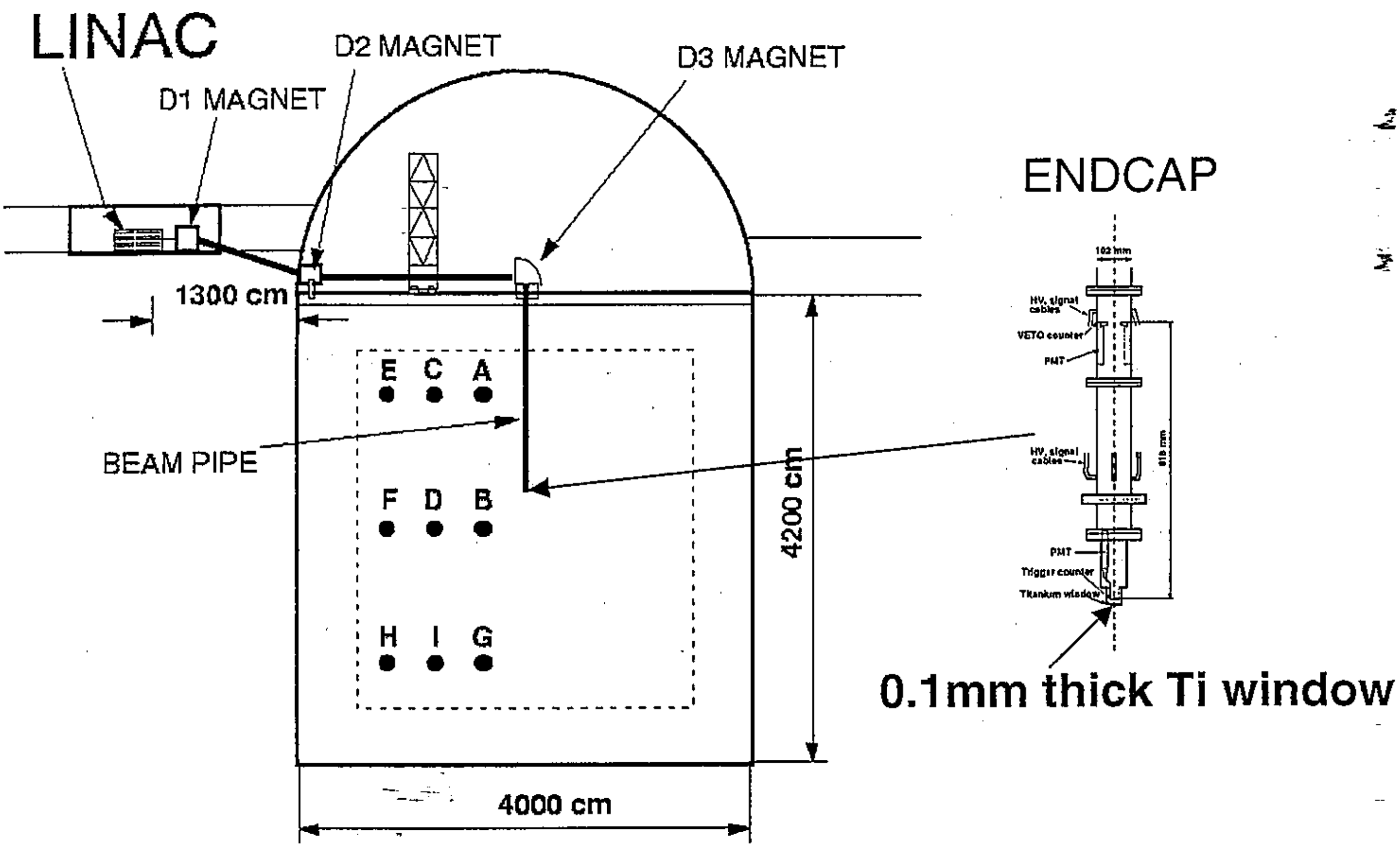

- Beam energy: 5 ~ 16 MeV/c
- Beam energy spread: < 0.5 %
- Data taking at 9 typical positions in SK
- Beam energy determined by Ge detector (<20 keV accuracy)

Energy spectrum of LINAC calibration

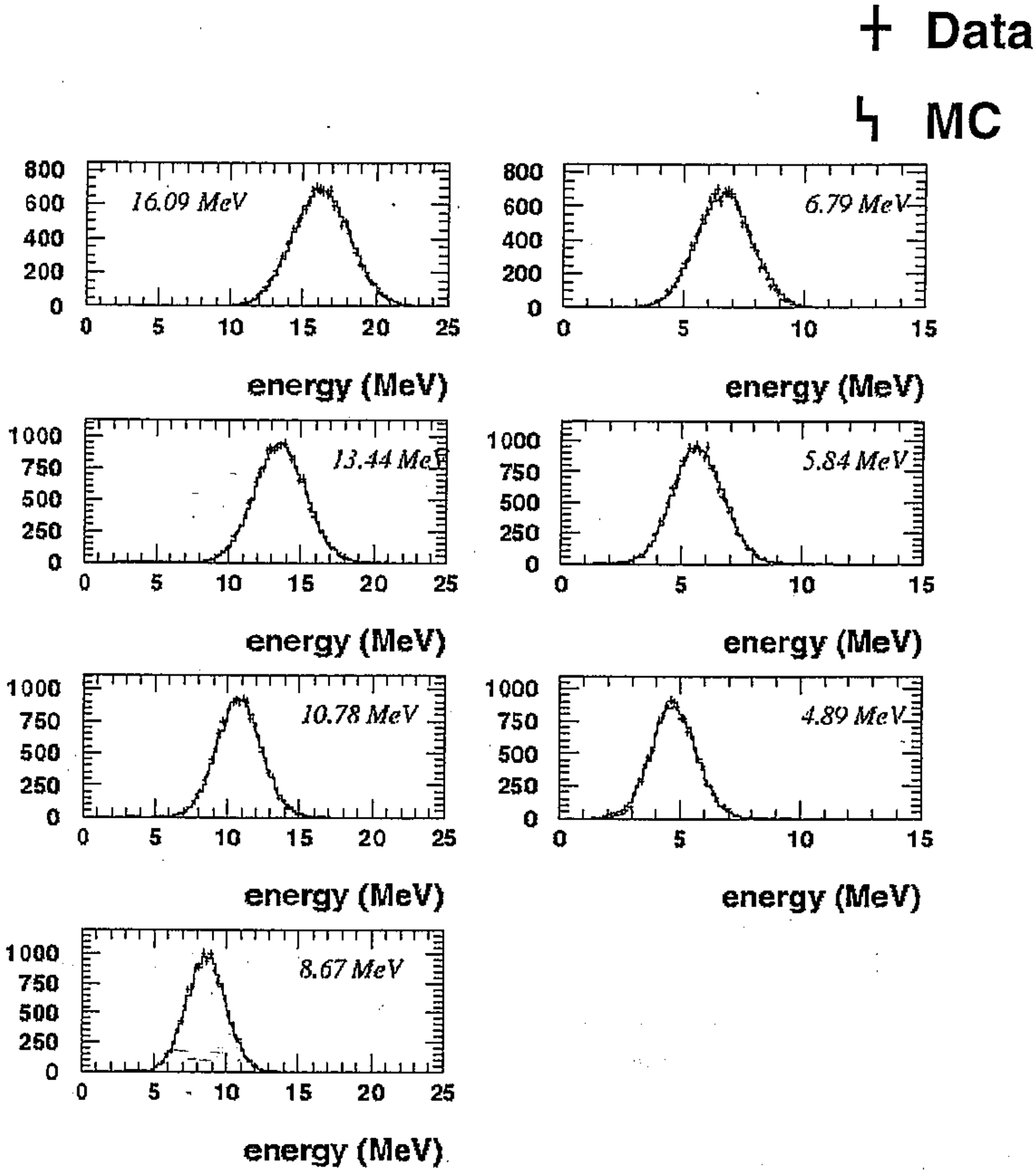

Energy scale and resolution are precisely calibrated.

Systematic error of the absolute energy scale is 0.64 %.

Error in energy scale or resolution

LINAC calibration

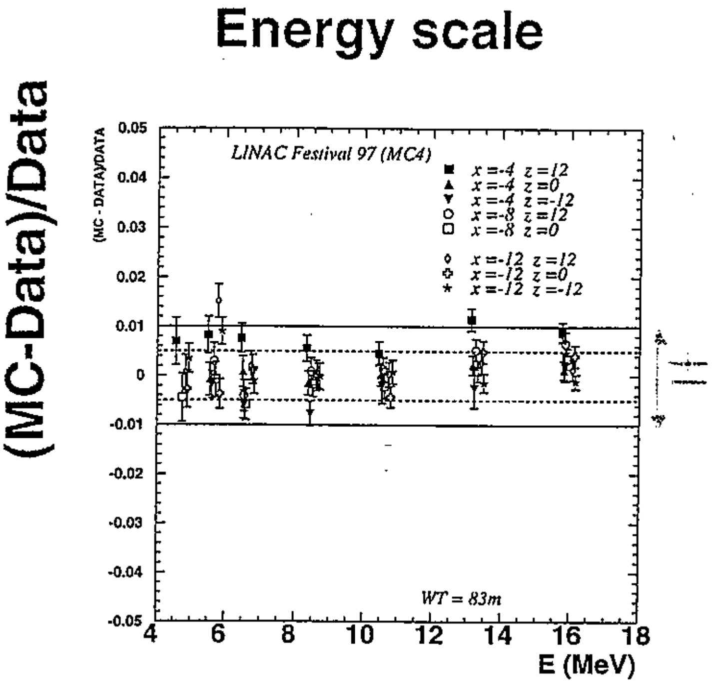

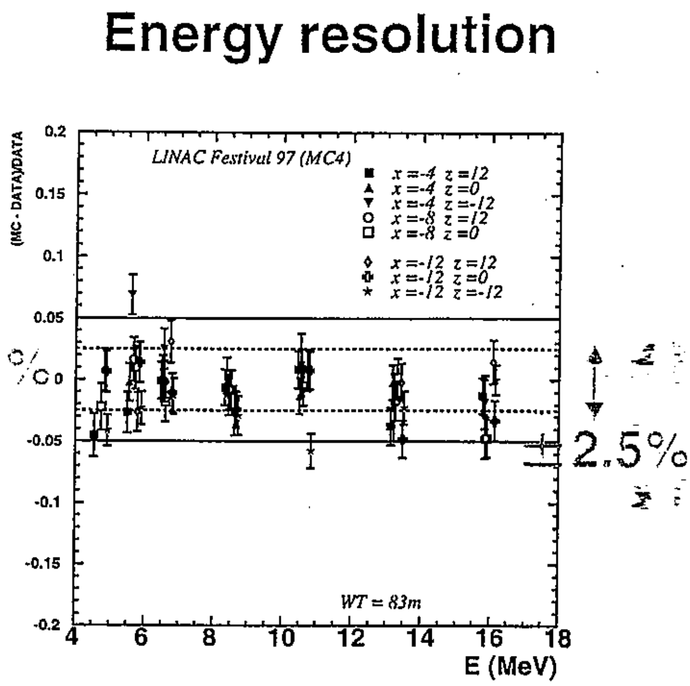

Resolution tail ?

LINAC 10.78 MeV data

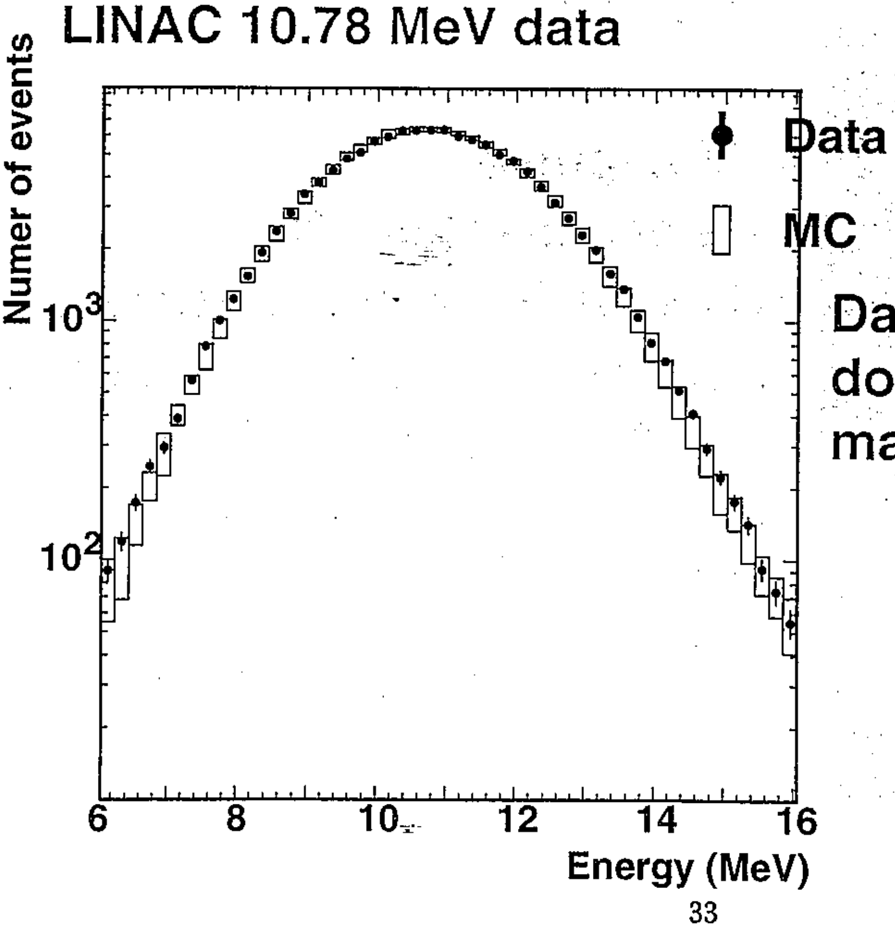

Data and MC agree down to 2 orders of magnitudes

^{16}N calibration

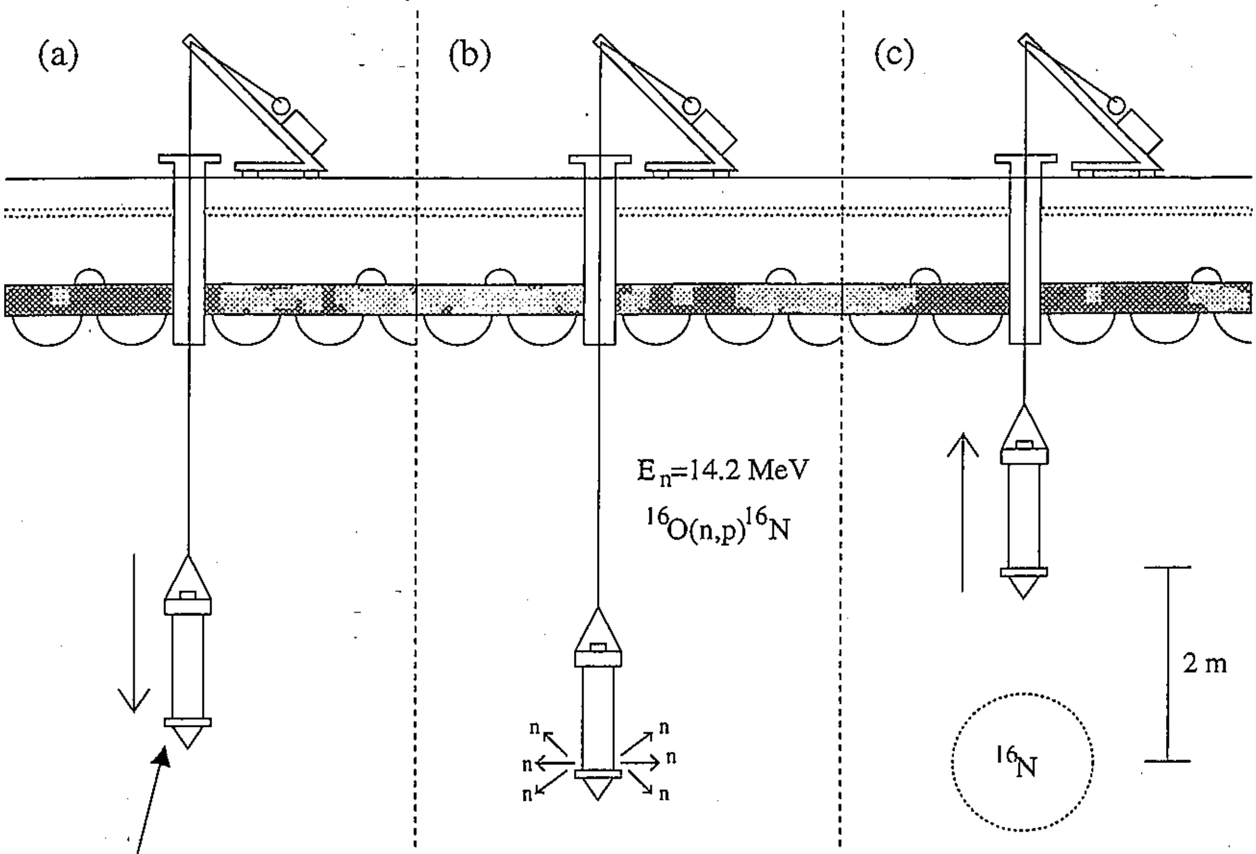

DT generator

$D+T \rightarrow He+n$ (14.2 MeV) $n+{}^{16}O \rightarrow p+{}^{16}N$

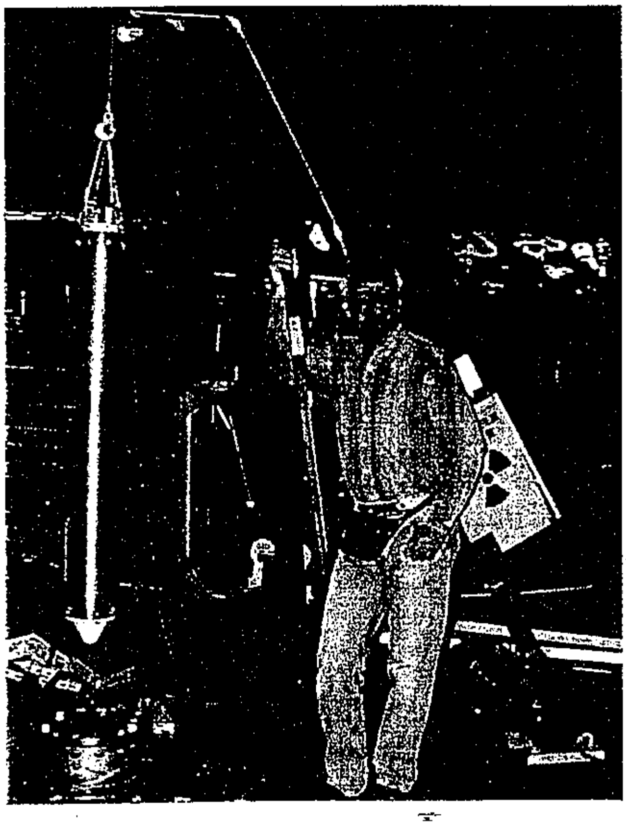

~10^6 n /pulse

~1% of n creates ^{16}N

^{16}N decay is precisely known.

66.2% 6.129MeVγ + 4.29MeVβ,

28.0% 10.419 MeV β, and etc.

Data taken at various positions in the detector.

Uniform direction complementary to LINAC calibration.

^{16}N calibration data

Event time after fire

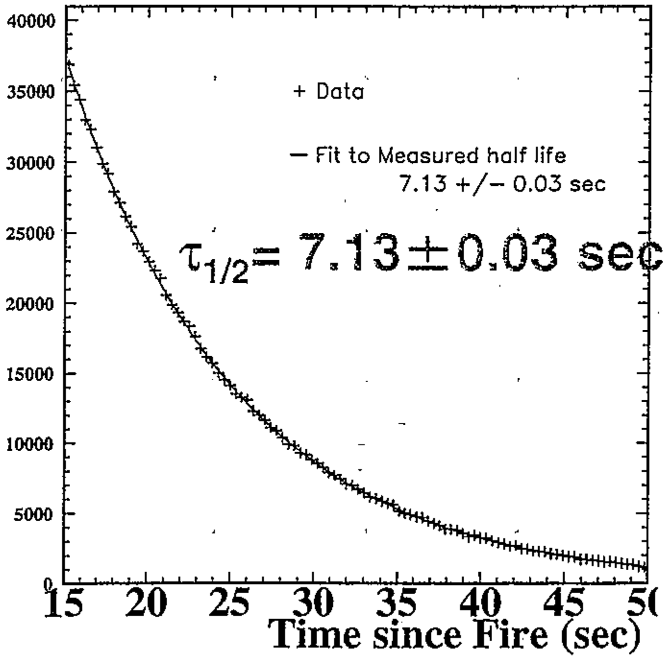

Energy spectrum

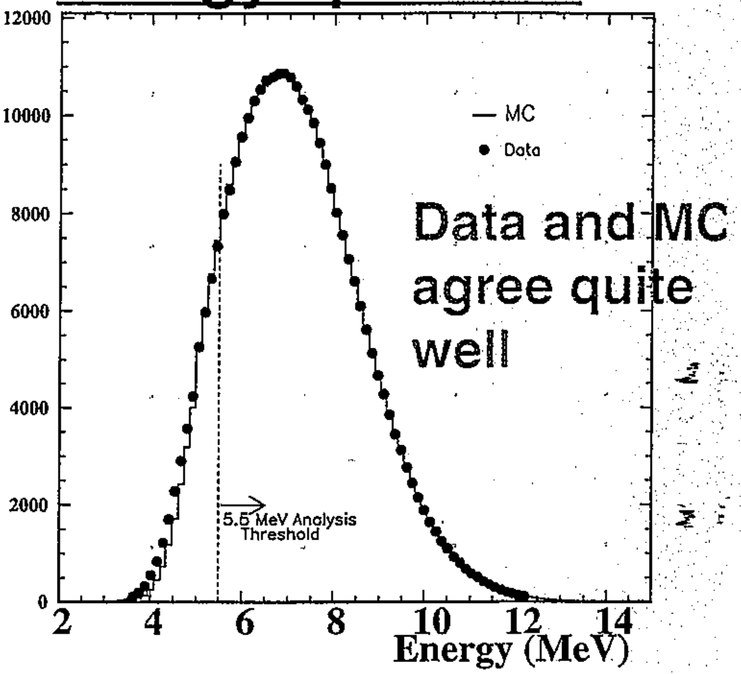

Direction dependence of energy scale

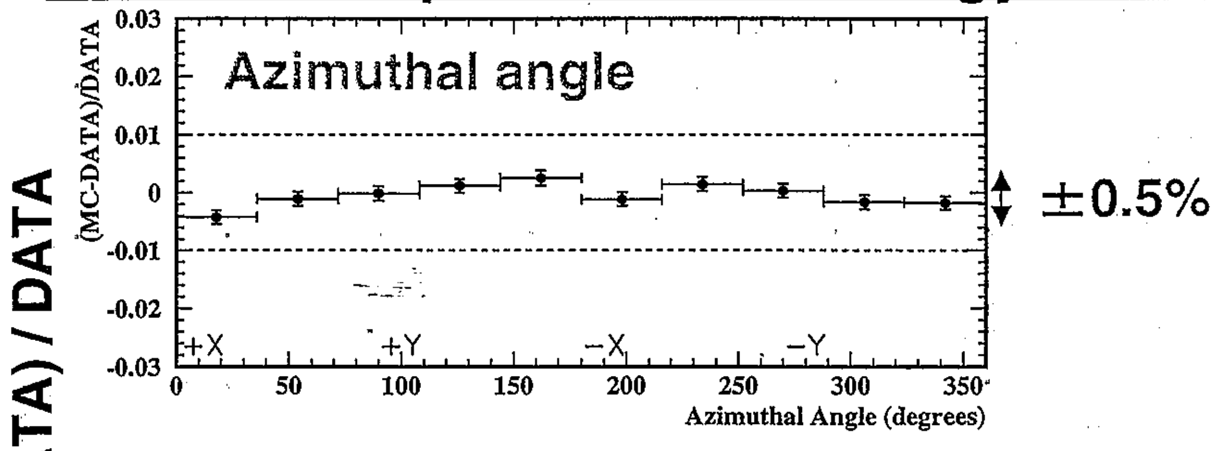

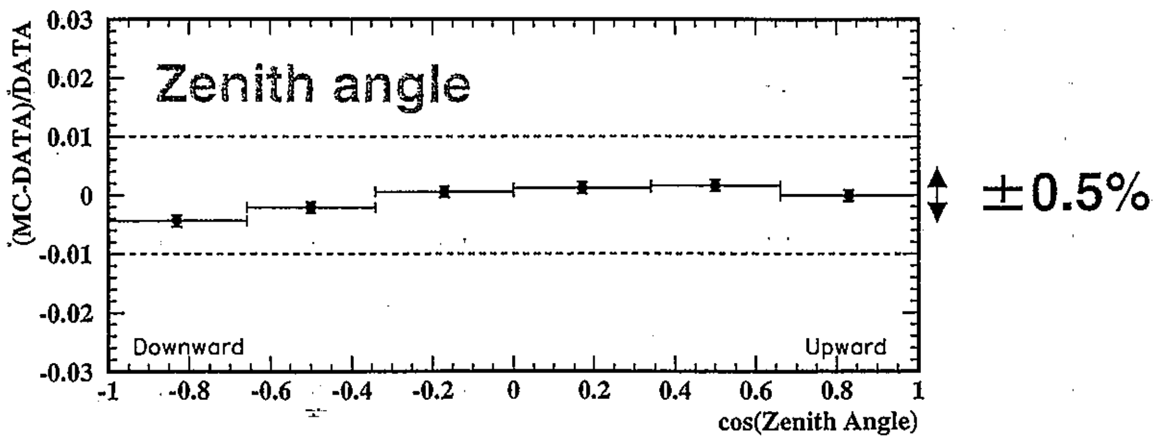

Water transparency and detector stability

Water transparency

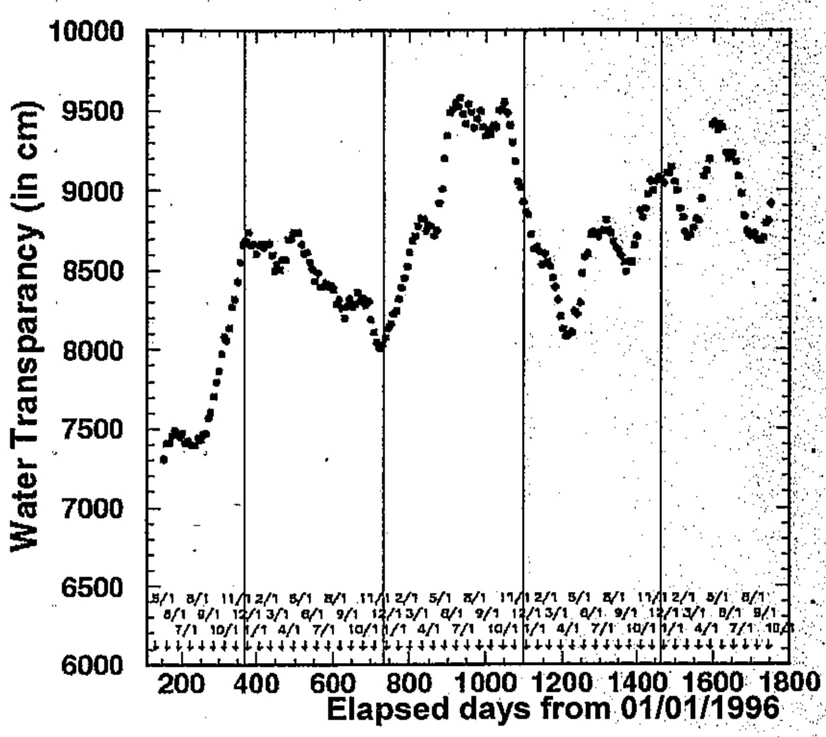

Spectrum mean of $\mu \rightarrow e$ decay

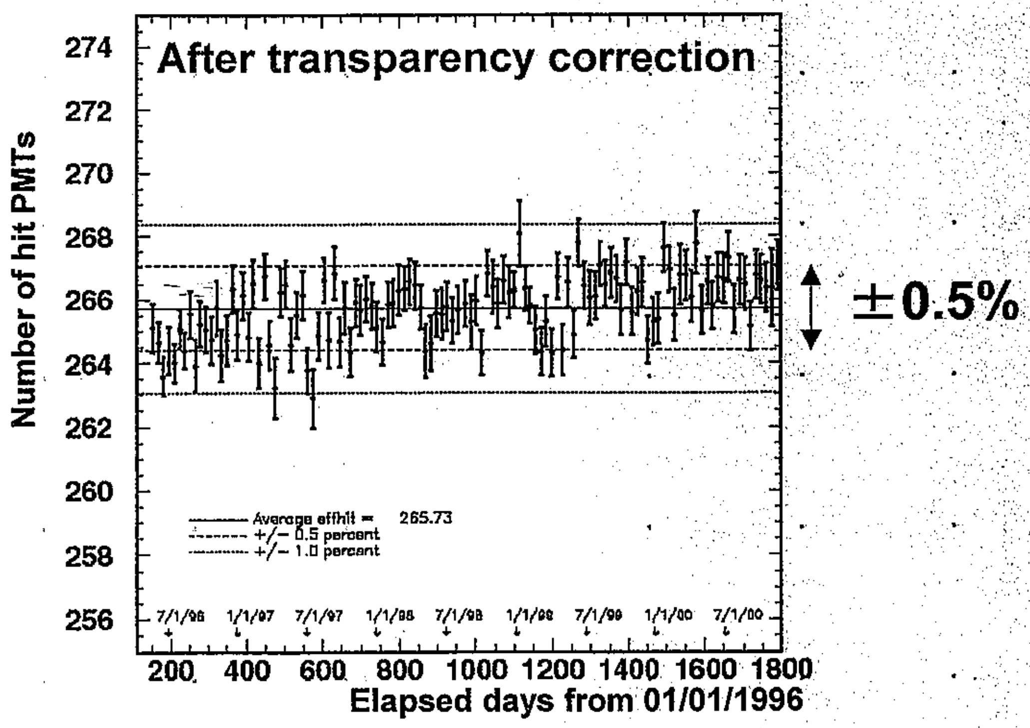

Absolute energy scale is stable within ±0.5 %.

Direction to the Sun

May 31, 1996 - Oct.6, 2000

1258 days

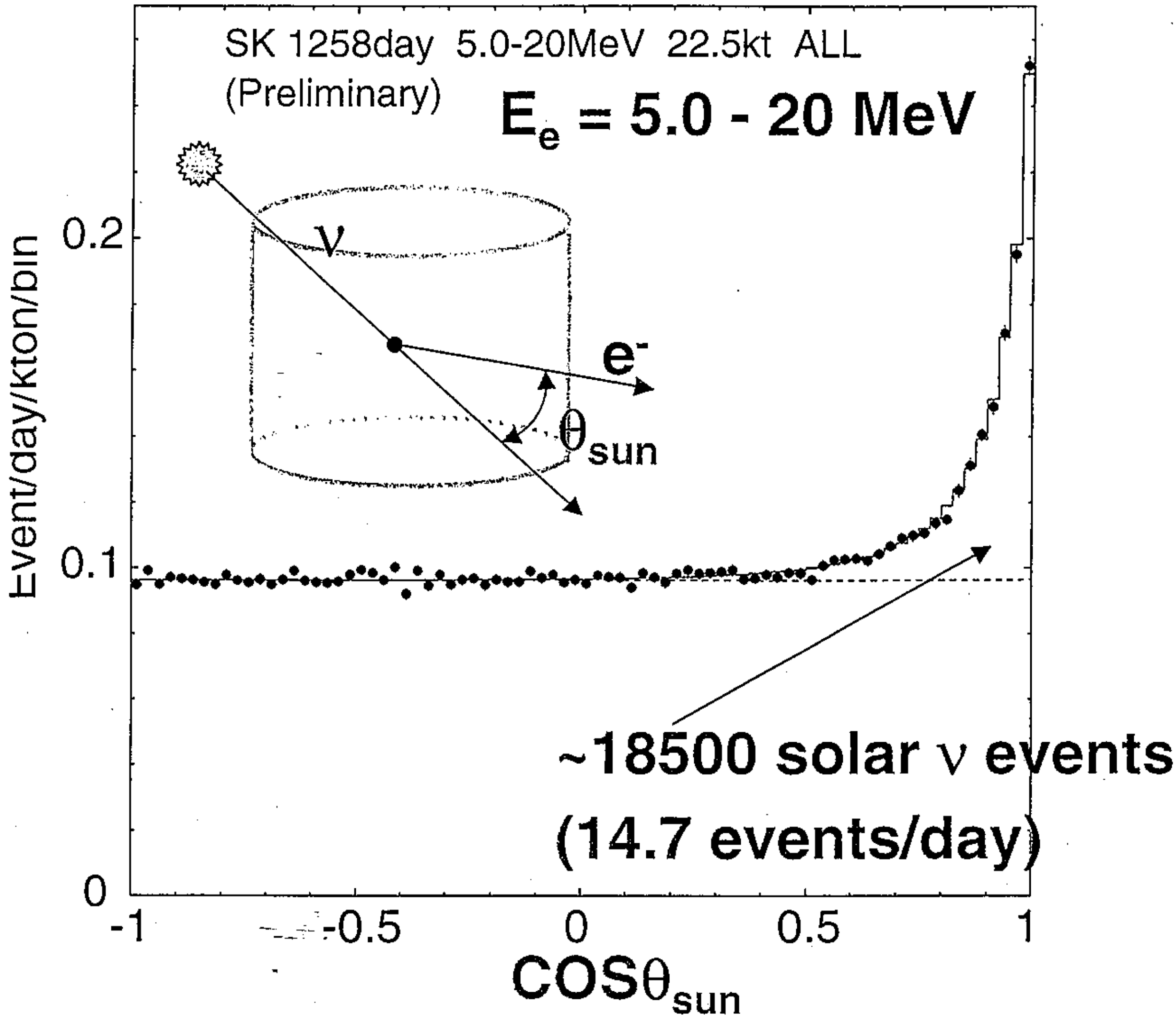

^{8}B flux : $2.32 \pm 0.03 \,^{+0.08}_{-0.07}$ [x 10^6 /cm^2/sec]

$$\frac{\text{Data}}{\text{SSM(BP2000)}} = 0.451 \pm 0.005 \,^{+0.016}_{-0.013}$$

→ 5.15×10^6/cm^2/sec

(using Ortiz et al. spectrum shape(nucl-ex/0003006))

(although recently updated to 5.05×10^6/cm^2/sec)

Direction to the Sun in Lower Energy Range

May 29, 1997 – Oct.6, 2000
978 days

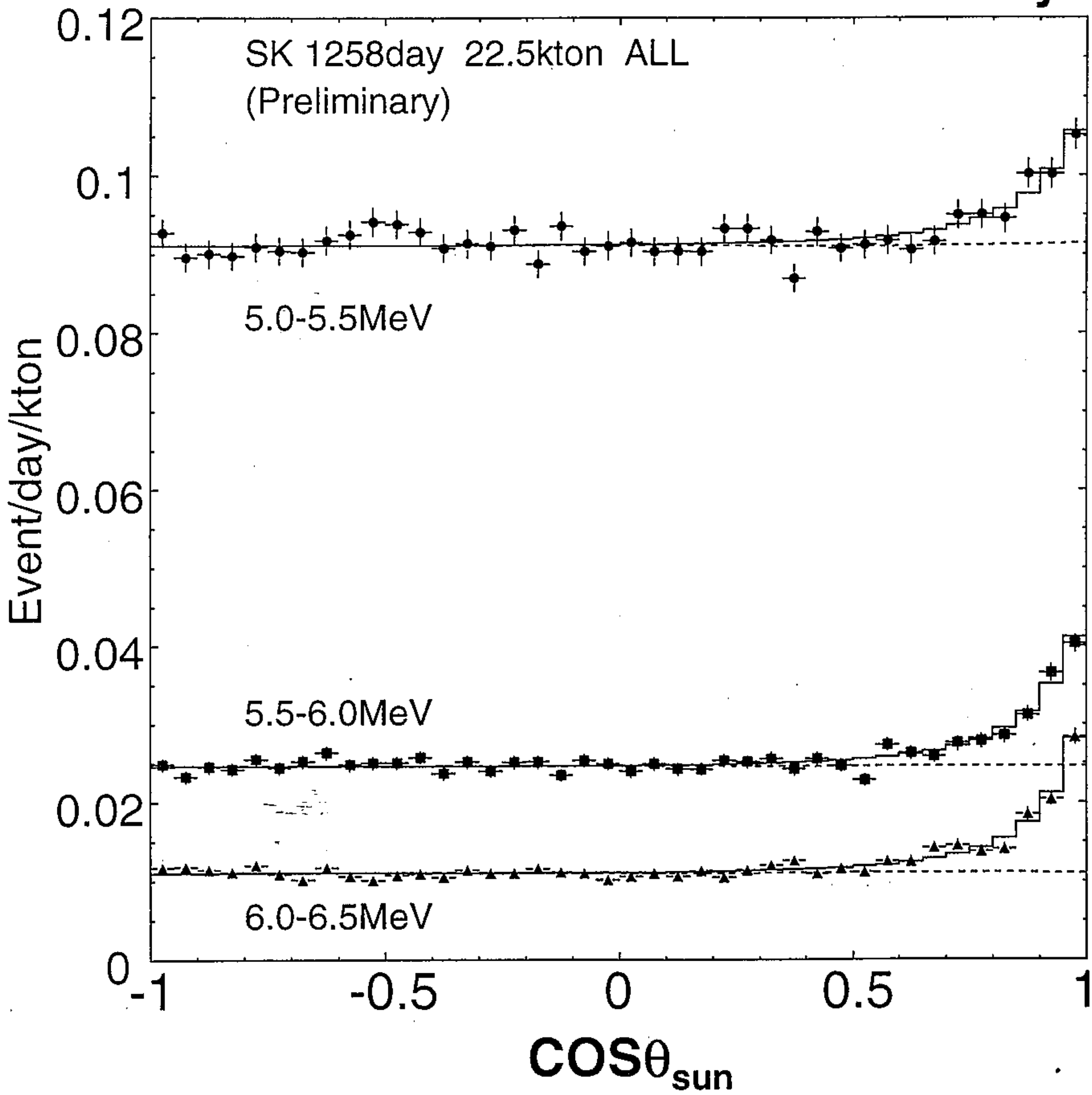

Time variation of the flux

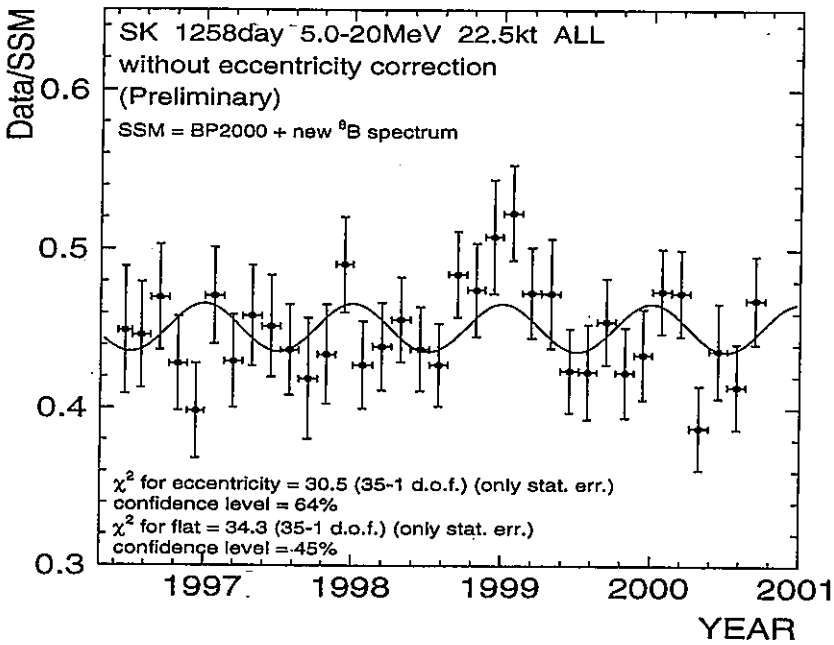

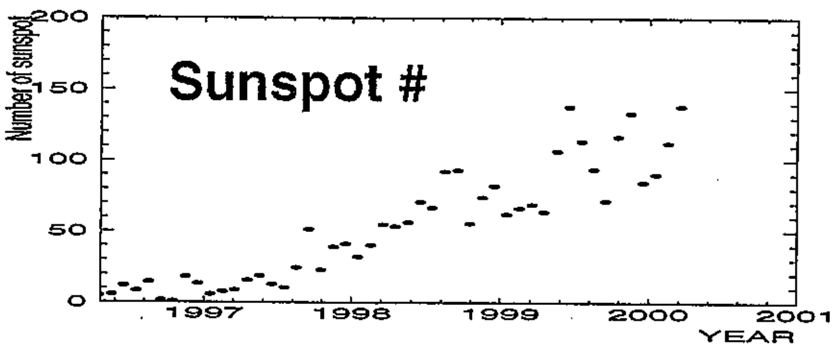

Seasonal variation of the flux

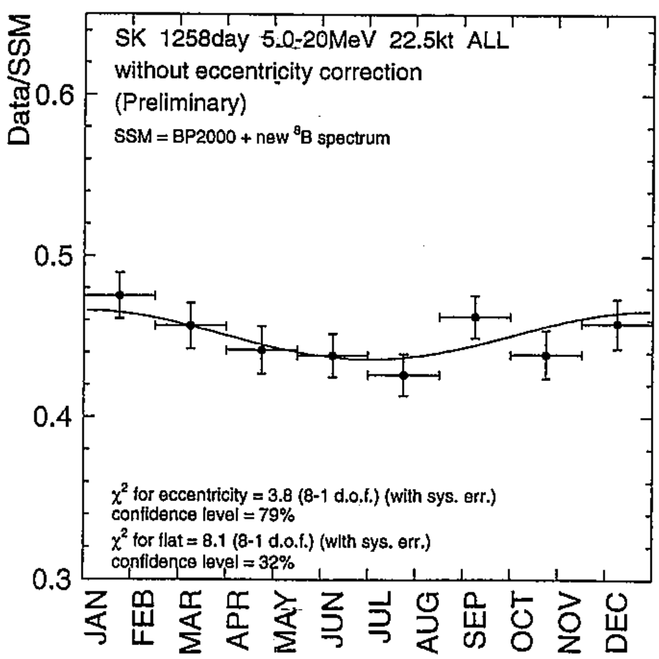

χ^2 for eccentricity: 3.9 / 7 d.o.f. (79% C.L.)

(χ^2 for flat: 8.1 / 7 d.o.f. (32% C.L.))

Day/Night Effect

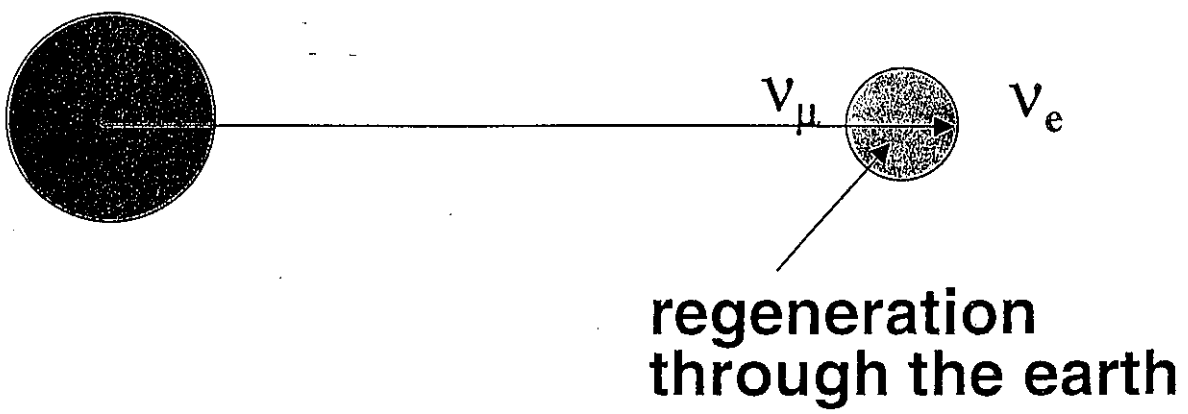

Earth density: ρ=5g/cm² (average), 13(at core)

Affect to oscillations for $\Delta m^2 = 10^{-6}$ - 10^{-4} eV²

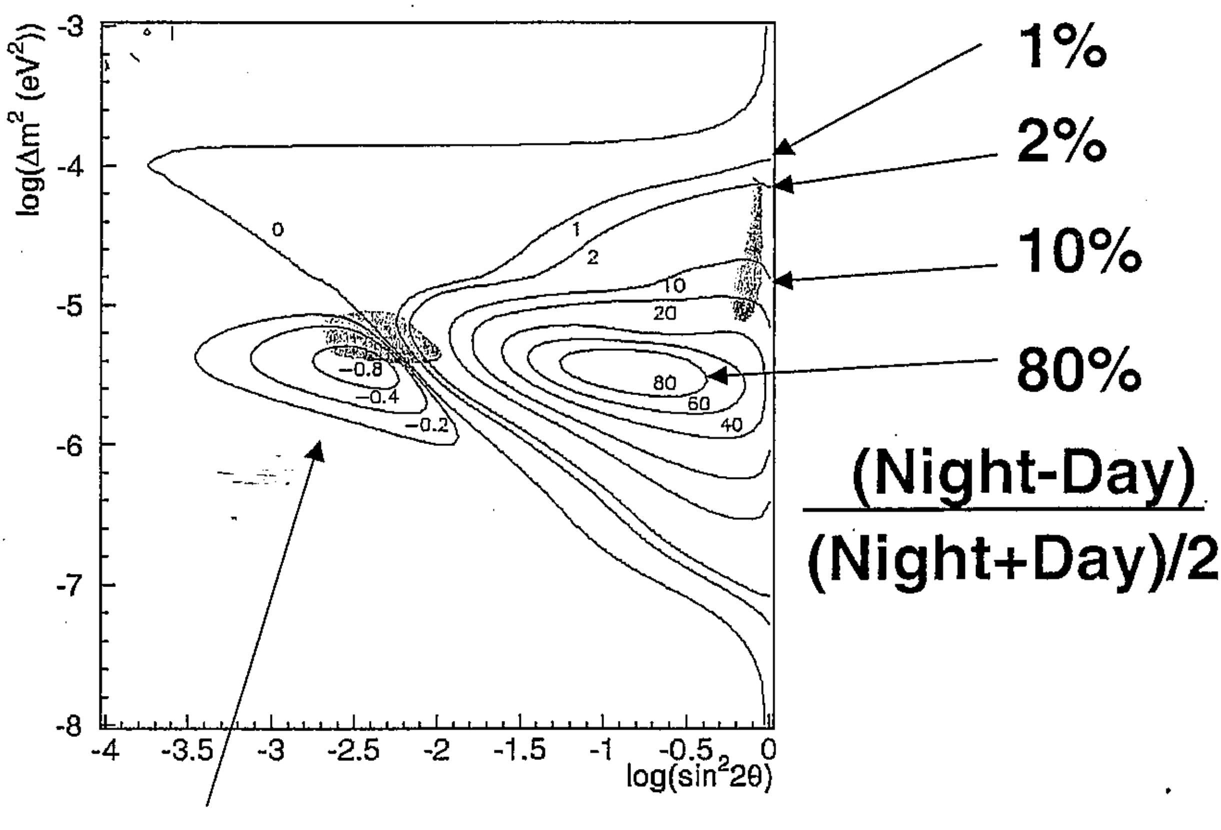

Day/Night analysis

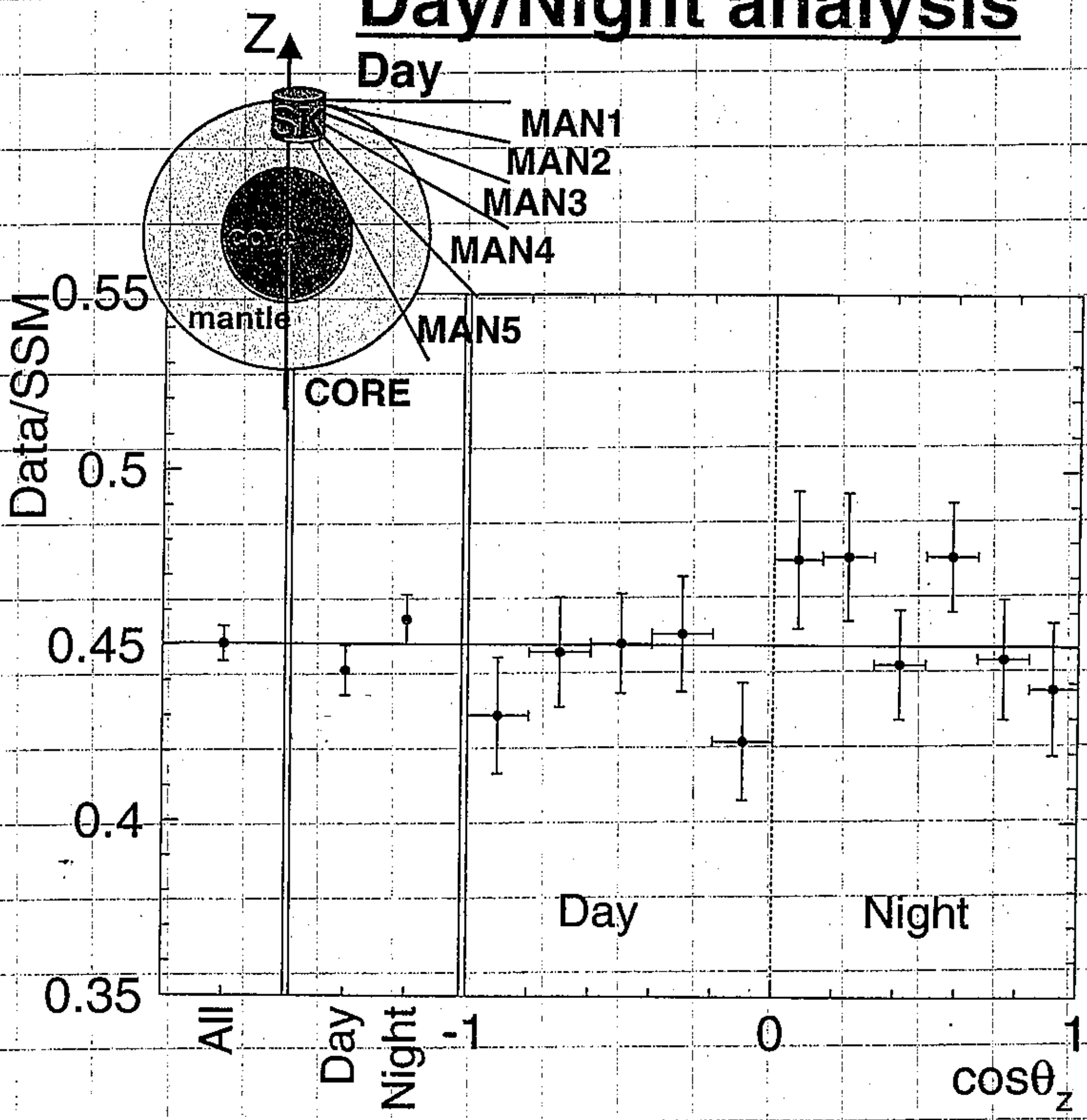

Day: 622 effective days

$$f(^8B) = 2.28 \pm 0.04 \pm^{0.08}_{0.07} [\times 10^6/cm^2/s]$$

Night: 636 effective days

$$f(^8B) = 2.36 \pm 0.04 \pm^{0.08}_{0.07} [\times 10^6/cm^2/s]$$

$$\frac{N-D}{(N+D)/2} = 0.033 \pm 0.022(\text{stat.}) \pm ^{0.013}_{0.012} (\text{sys.})$$

$\sim 1.3\sigma$ effect

Energy Spectrum

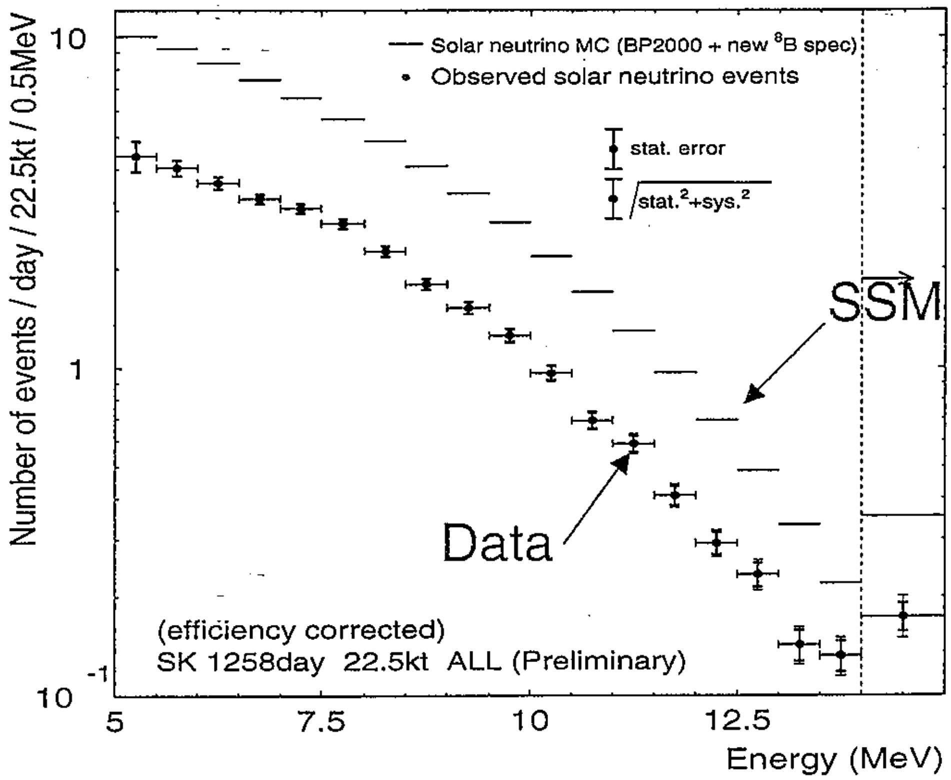

Data/SSM$_{BP2000}$

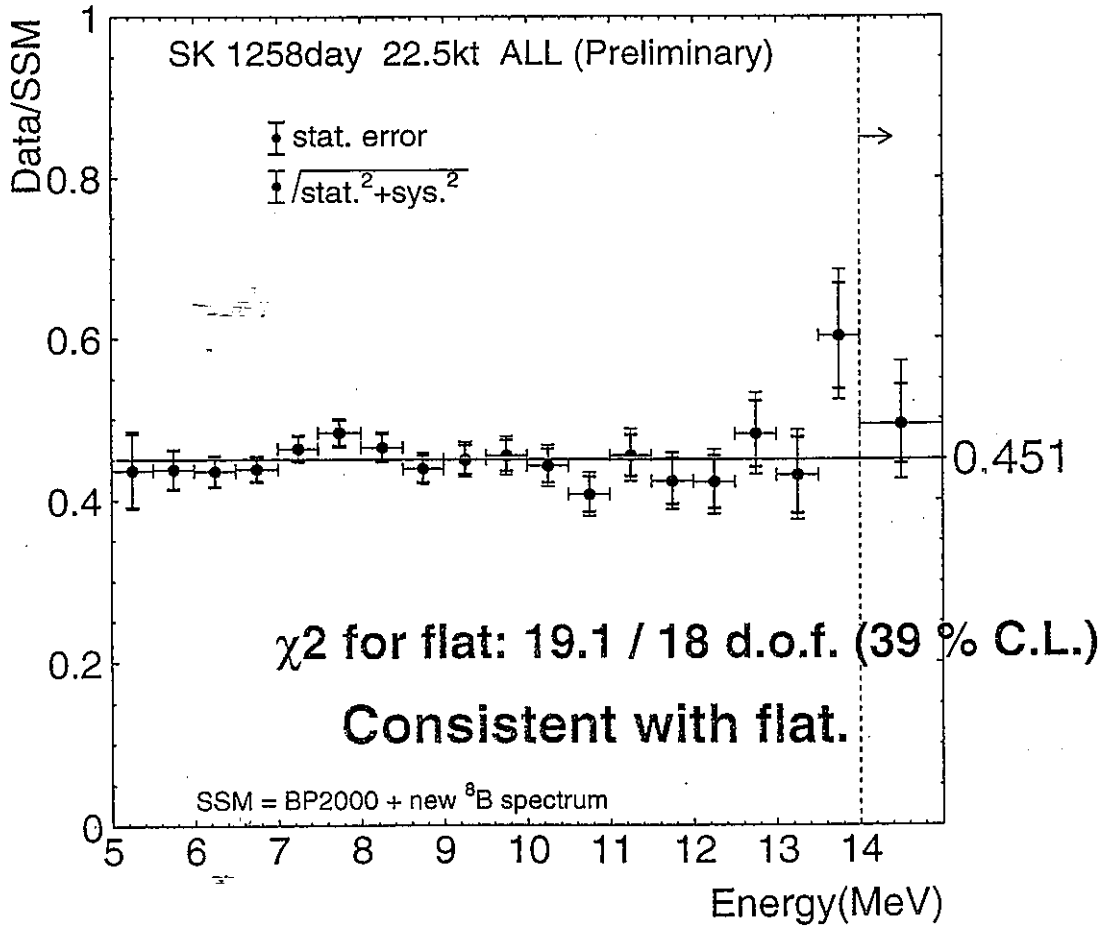

Expected ^{8}B neutrino spectrum shape

New measurement of α decay spectrum of ^{8}B decay by Ortiz et al. Phys. Rev.Lett.85(2000)2909).

^{8}B neutrino spectrum based on the new α spectrum

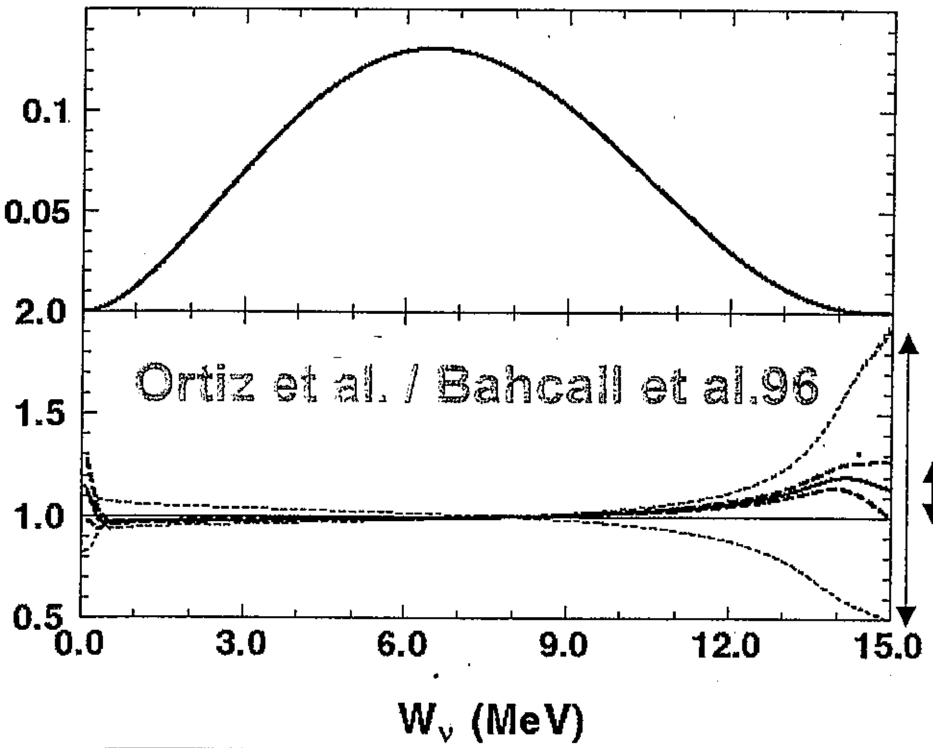

Ortiz et al. spectrum shape was adopted. But, error is conservatively Ortiz error + theoretical error.

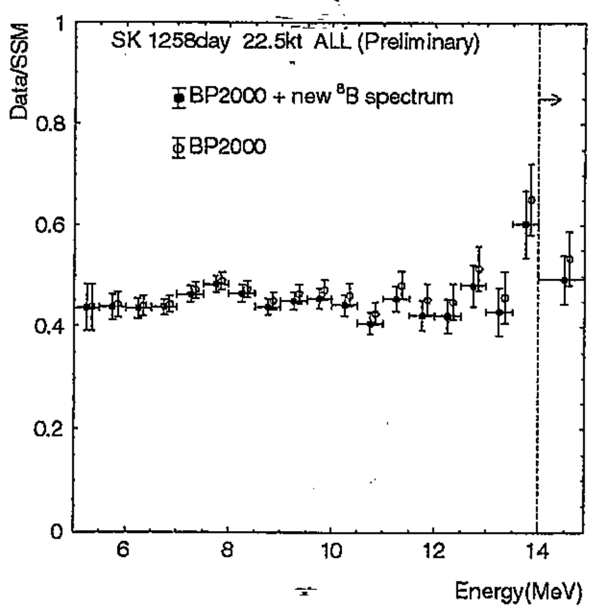

Difference in SK spectrum

- **Ortiz et al. spectrum**
- **Bahcall et al. 96 spectrum**

Shape of the ^{8}B Alpha and Neutrino Spectra

C. E. Ortiz,[1] A. García,[1,2] R. A. Waltz,[1] M. Bhattacharya,[1,*] and A. K. Komives[1]
[1] *University of Notre Dame, Notre Dame, Indiana 46556*
[2] *Lawrence-Berkeley National Laboratory, Berkeley, California 94720*
(Received 15 March 2000)

The β-delayed α spectrum from the decay of ^{8}B has been measured with a setup that minimized systematic uncertainties that affected previous measurements. Consequently the deduced neutrino spectrum presents much smaller uncertainties than the previous recommendation [J. N. Bahcall *et al.*, Phys. Rev. C 54, 411 (1996)]. The ^{8}B ν spectrum is found to be harder than previously recommended with about (10–20)% more neutrinos at energies between 12–14 MeV. The integrated cross sections of the ^{37}Cl, ^{71}Ga, ^{40}Ar, and Super-Kamiokande detectors are, respectively, 3.6%, 1.4%, 5.7%, and 2.1% larger than previously thought.

PACS numbers: 23.40.Bw, 23.60.+e, 26.65.+t, 27.20.+n

The solar neutrino detectors Super-Kamiokande, SNO, and ICARUS are sensitive primarily to neutrinos from the decay $^8\text{B} \rightarrow {}^8\text{Be} + e^+ + \nu_e$. The expected differences between the shape of this neutrino spectrum in the laboratory and in the sun are small [1]. Hence any observed difference between the shape of this spectrum as measured in the laboratory compared to that measured by solar neutrino detectors would imply nonstandard physics. For example, when the spectrum from Super-Kamiokande is compared to the expected spectrum based on laboratory measurements [2], one observes not just an overall reduction in the number of neutrinos but also a distortion of the spectrum; shape. Given the importance of an accurate knowledge of the shape of the ^{8}B neutrino spectrum, this state of affairs is unsatisfactory.

A common problem encountered by the previous measurements of the delayed-α spectrum is the energy summing of the α's with the preceding β^+'s, resulting in a distortion of the spectrum. In order to minimize this effect previous authors used small-solid-angle detectors. In addition, measuring the spectrum in singles, as was done by previous authors, entails subtracting low-energy β^+ backgrounds and possible events originating from ^{8}B's implanted in the frame of the catcher foil, correcting for shifts

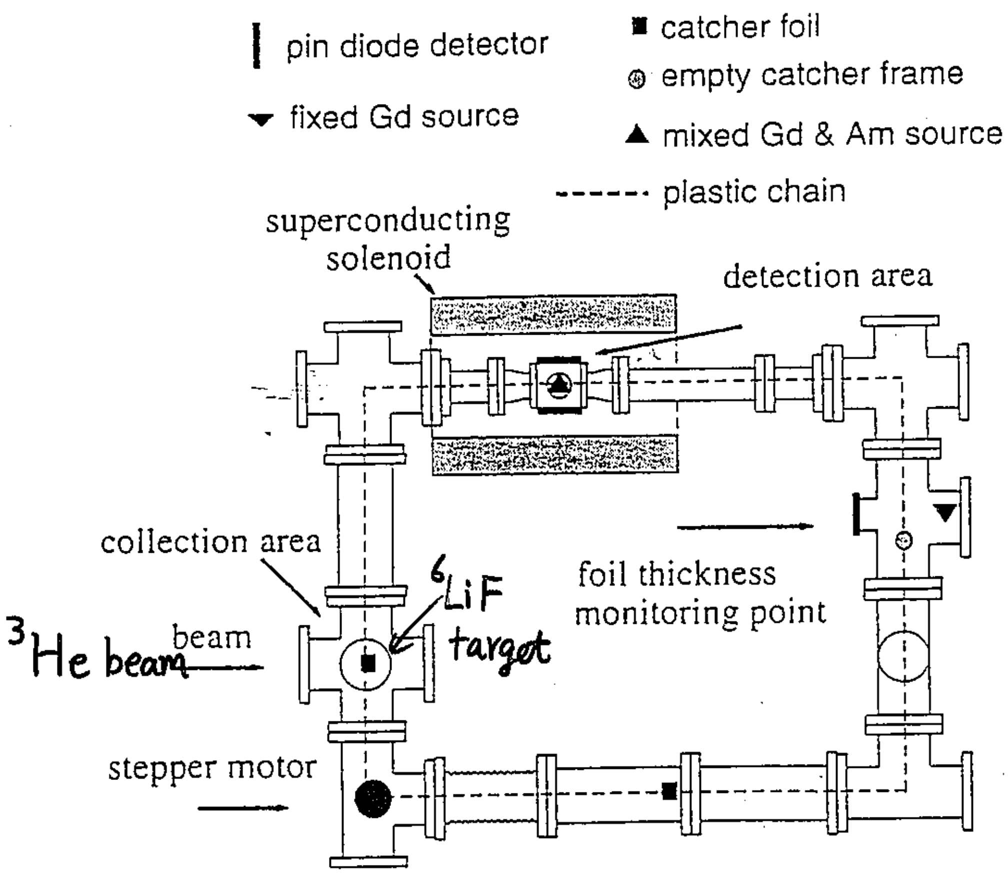

FIG. 1. Overhead view of the experimental setup.

Oscillation analysis

Spectrum shape comparison

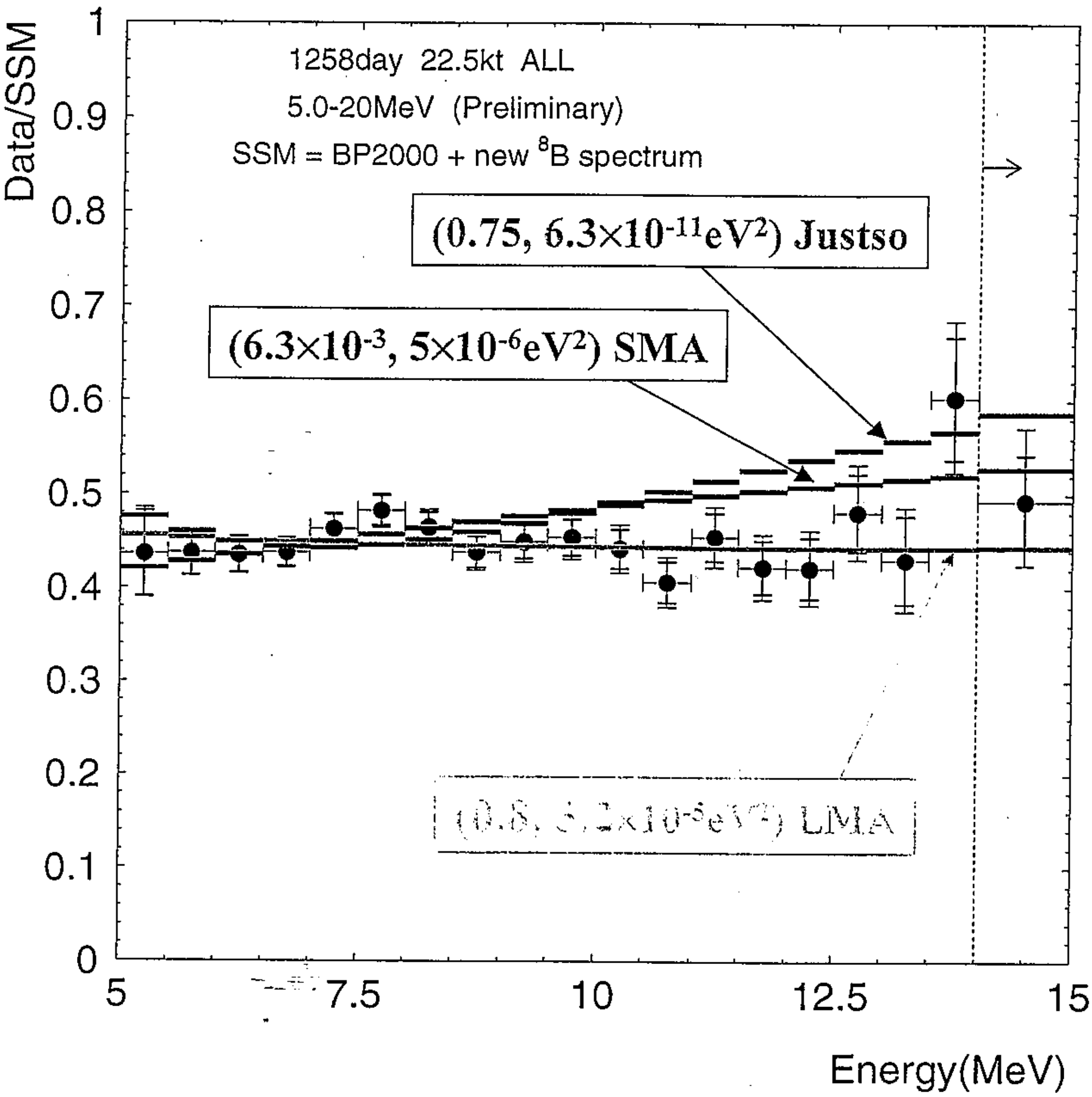

Bad fit for SMA and Just-so solutions.

Energy correlated systematic error

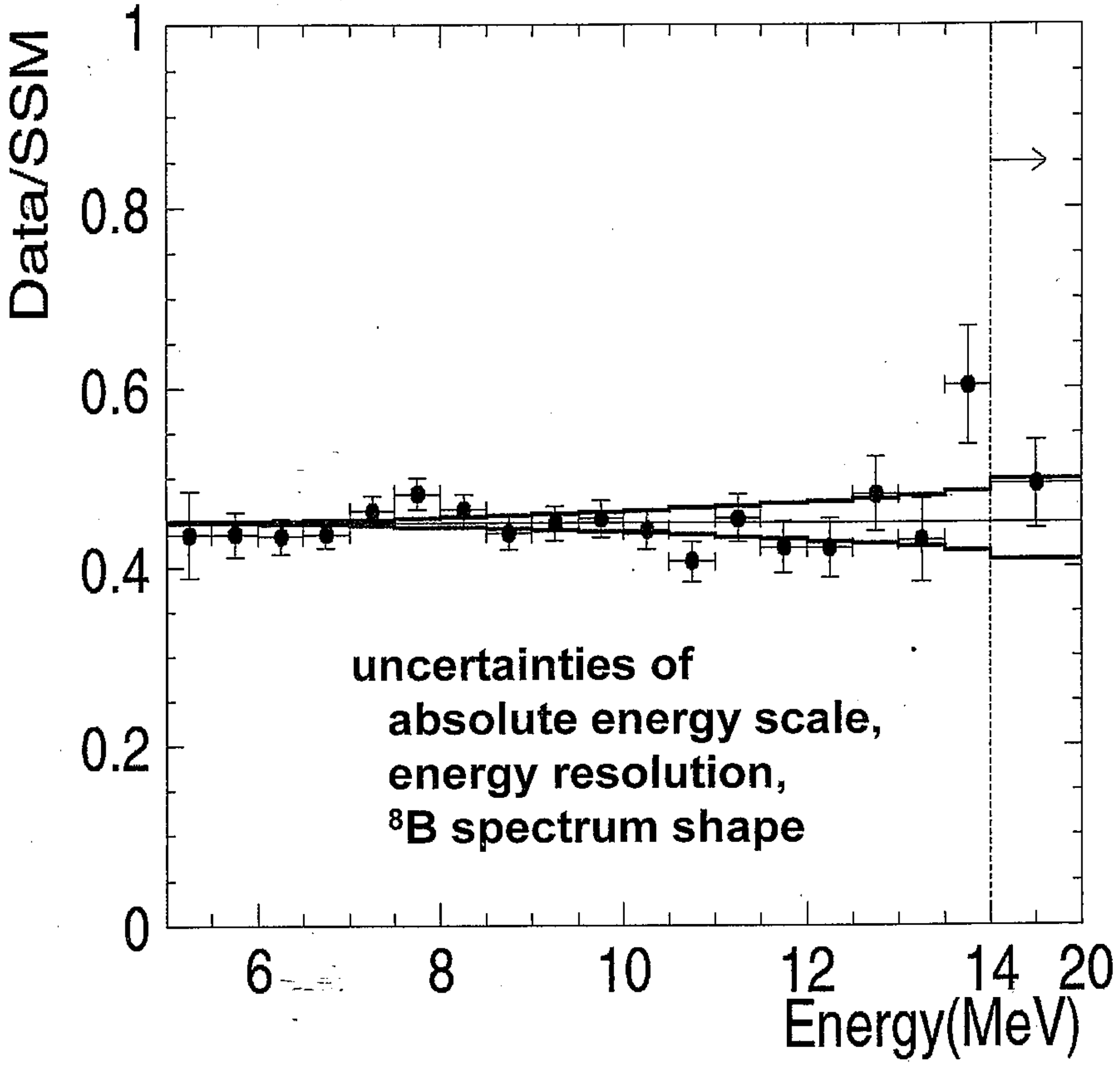

Energy distribution for day/night-6bins

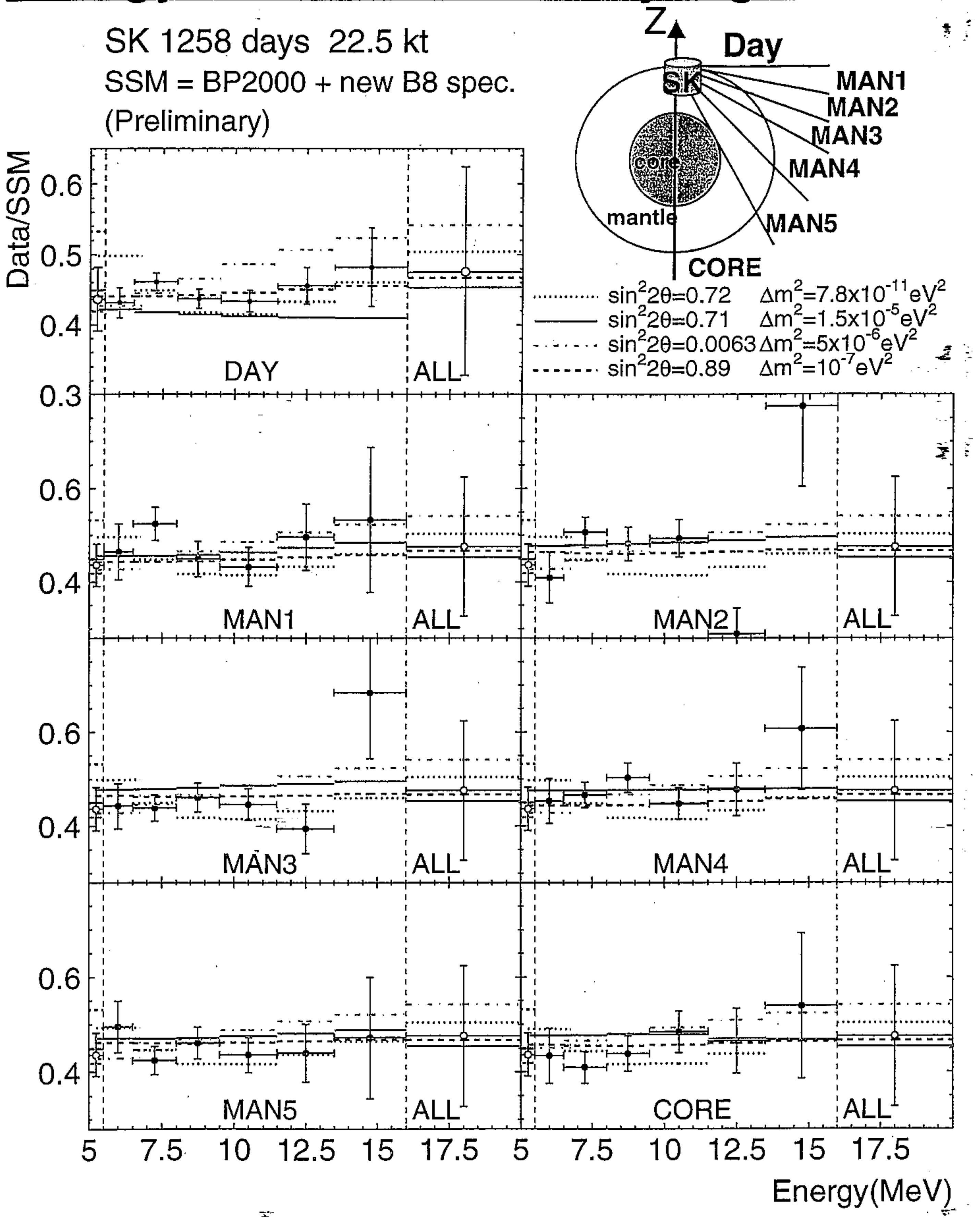

Variation Matrix (in zenith angle)

Deviation Vector (in zenith angle)

$$\chi^2 = \sum_{i=1}^{8} \vec{\Delta}_i^T \cdot V_i^{-1} \cdot \vec{\Delta}_i + \left(\frac{\delta_{\text{corr}}}{\sigma_{\text{corr}}}\right)^2 + \left(\frac{1-\alpha}{\sigma_{\text{flux}}}\right)^2$$

Energy bin

Correlated Uncertainty Deviation

Flux Normalization

SK measured Flux

Oscillated SSM Flux

$$\left(\vec{\Delta}_i\right)_z = \frac{\phi_{i,z}^{\text{meas}}}{\phi_i^{\text{SSM}}} - \frac{\phi_{i,z}^{\text{osc}}(\text{hep})}{\phi_i^{\text{SSM}}} \times f(E_i, \delta_{\text{corr}}) \times \alpha$$

free

Standard Solar Model Flux

Energy-correlated Uncertainty shape

$$V_i = V_i(\text{stat.}) + V_i(\text{E-uncorr.})$$

full correlation in zenith angle
zero correlation in energy

last term for flux-constraint fit only!

Oscillation analysis (SK vs. global, active)

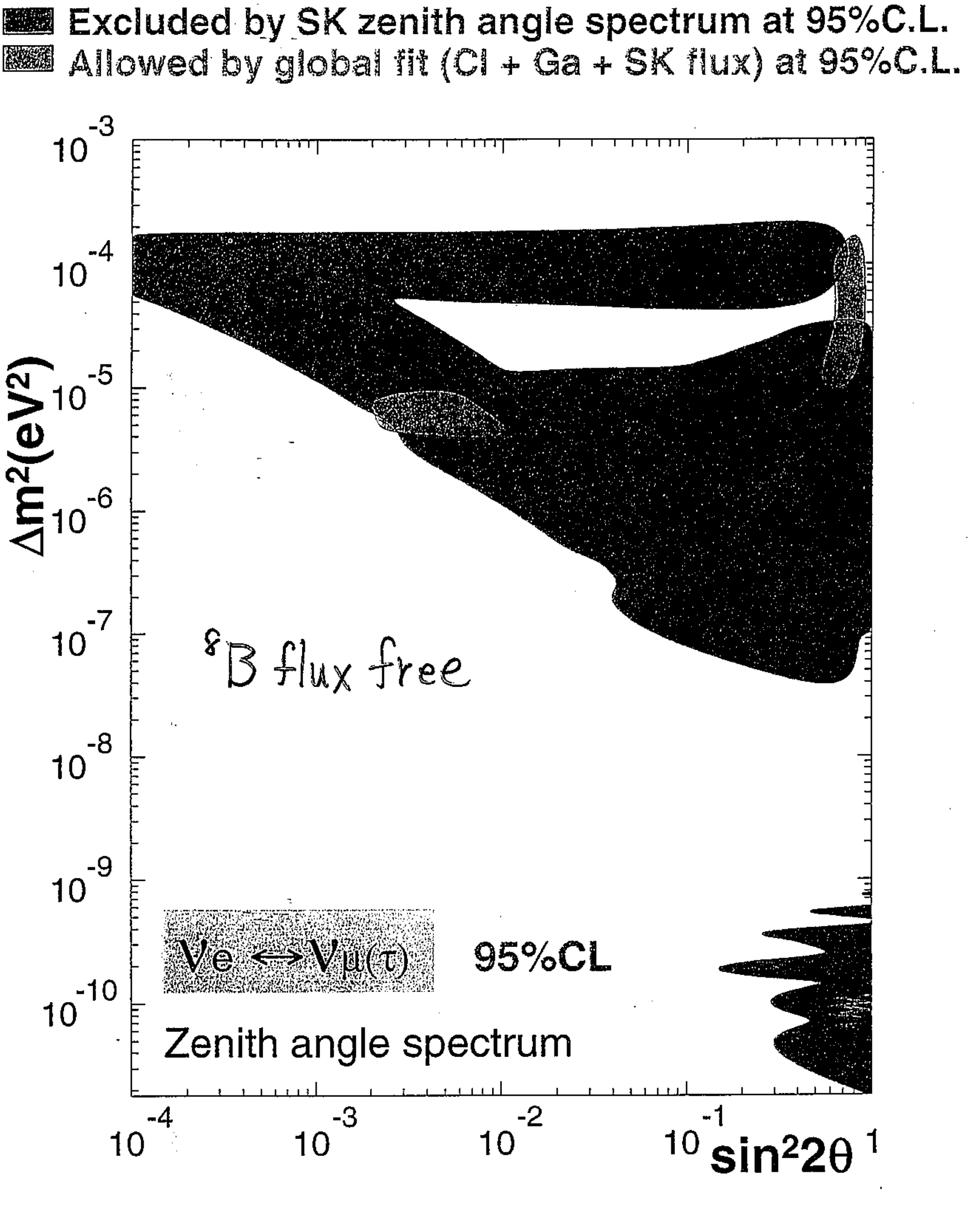

SMA & VAC solutions are disfavored at ~95% C.L. by comparing global fit and SK zenith spectrum

How SMA region is sensitive

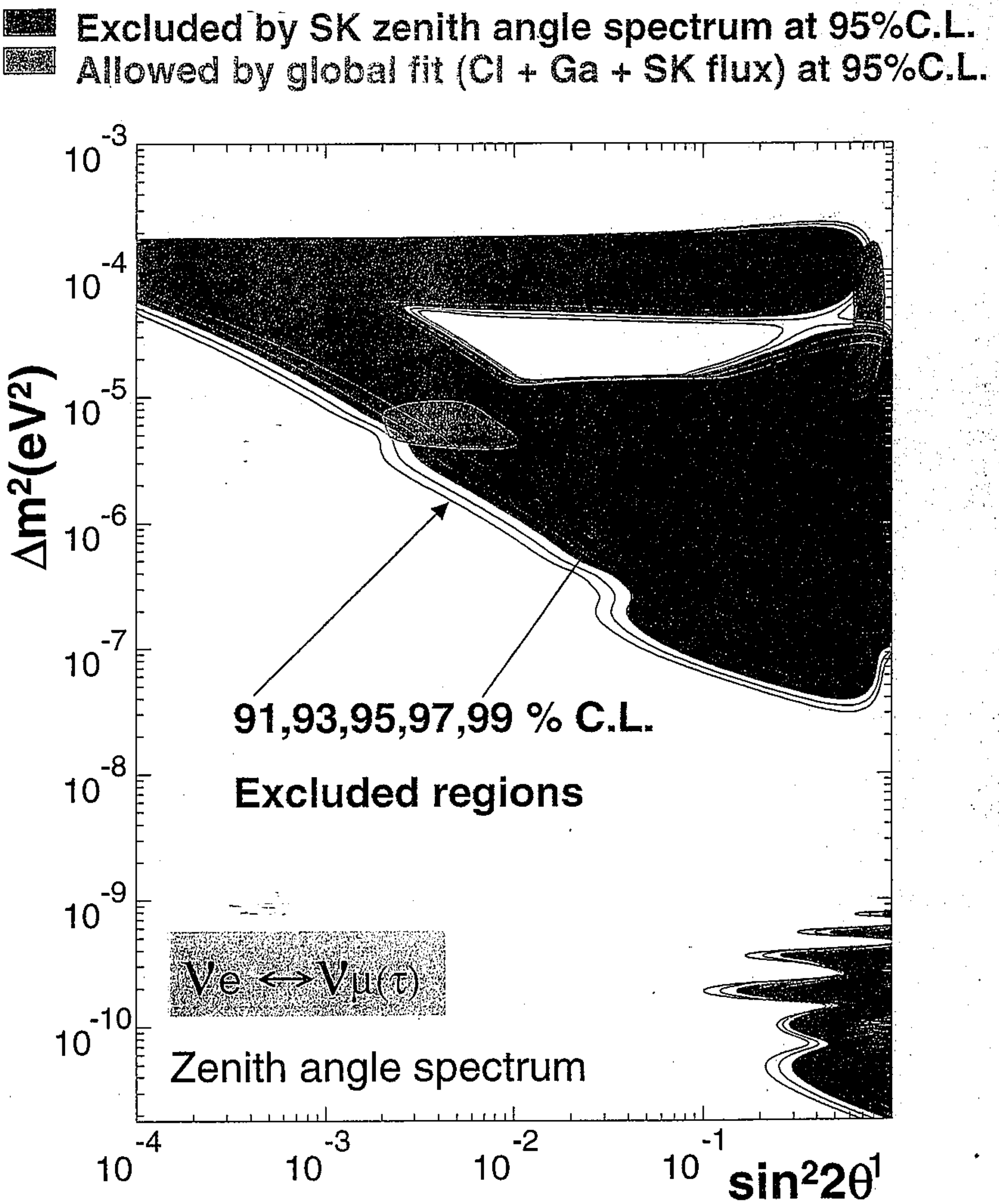

Confidence level at SMA region changes rather rapidly.

α (flux normalization factor) in the fit

$\nu_e \leftrightarrow \nu_{\mu(\tau)}$ Zenith angle spectrum

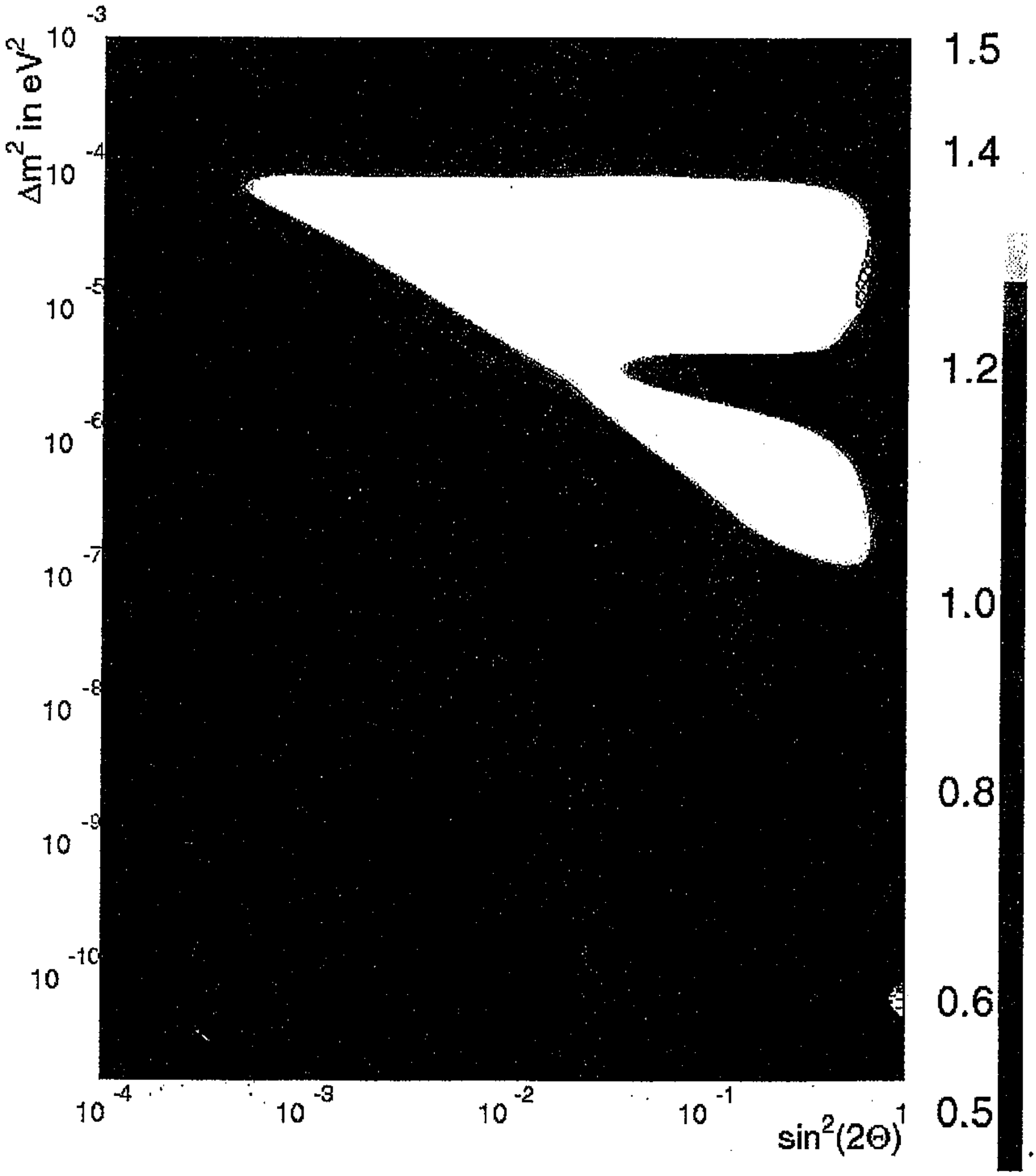

SMA requires lower value of α and LMA requires nearly α = 1.

+20% 1σ flux error
-16% in SSM

Oscillation analysis (flux constraint, active)

■ Allowed by SK zenith angle spectrum & flux at 95%C.L.

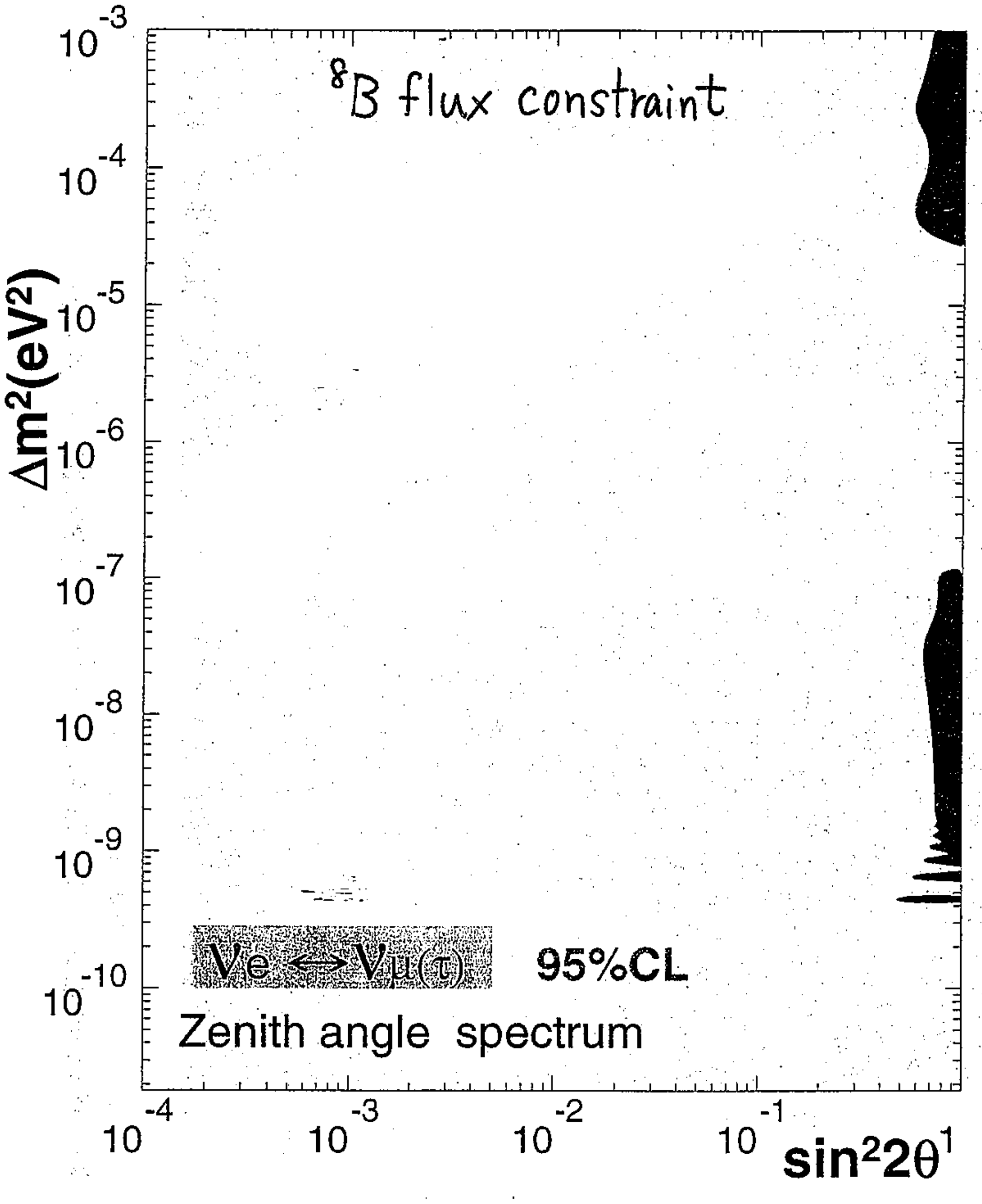

Large mixing is favored by SK d/n spectra with flux constraint (SK data only)

Oscillation analysis (flux constraint, active)

Allowed by SK zenith angle spectrum & flux at 95%C.L.

Allowed by global fit (Cl + Ga + SK flux) at 95%C.L.

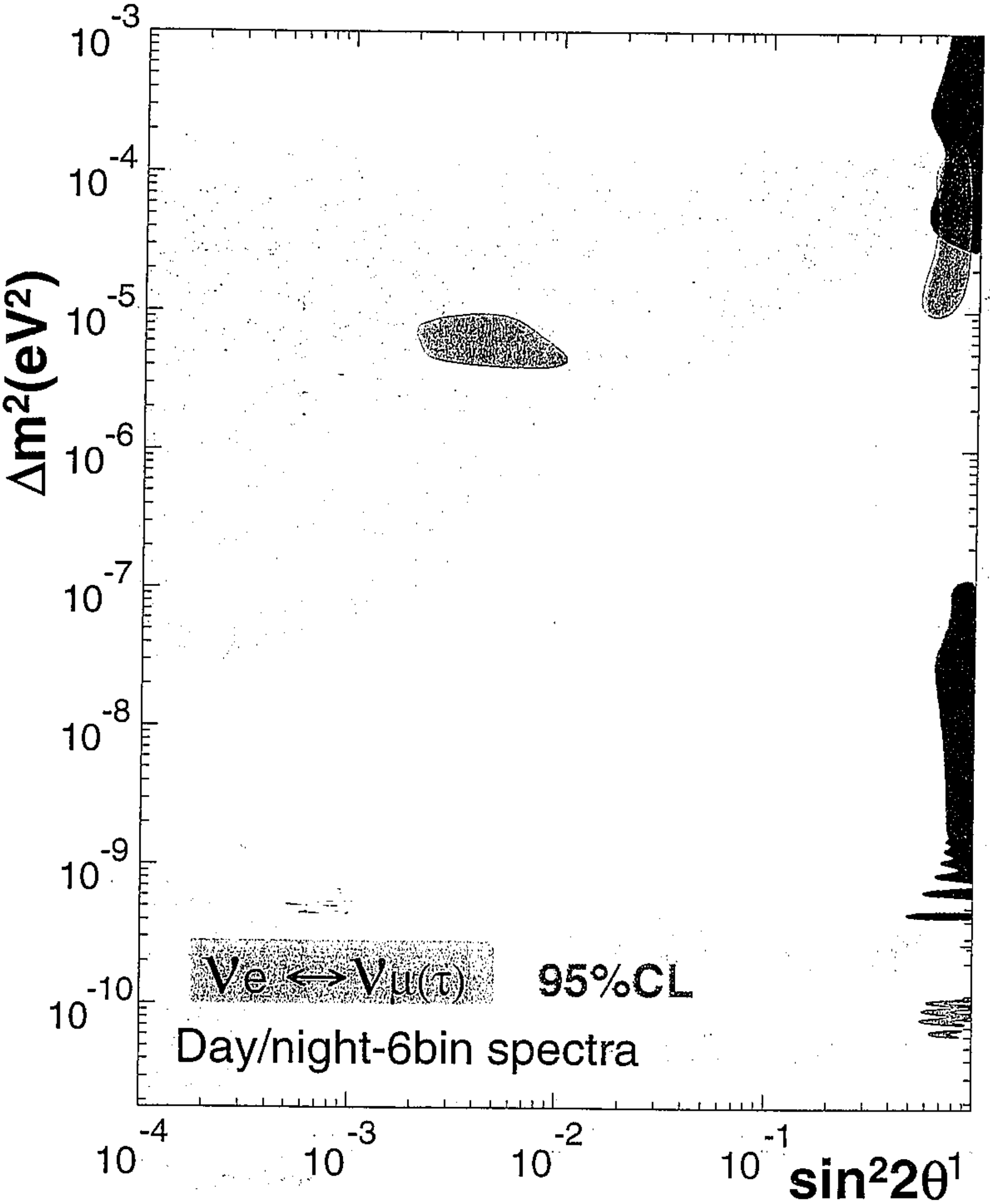

Large mixing is favored by SK d/n spectra with flux constraint (SK data only)

Oscillation analysis (SK vs. global, sterile)

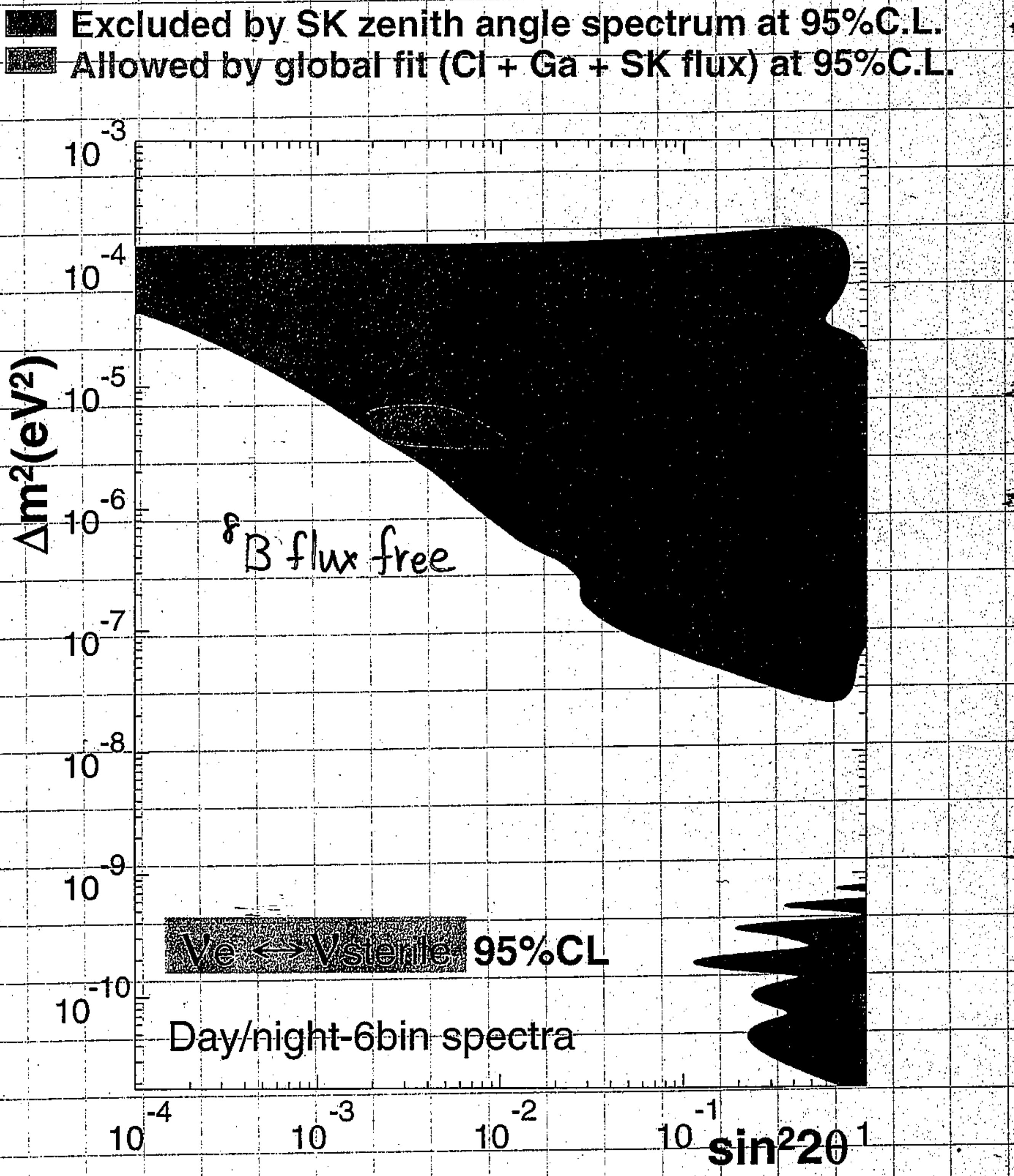

2-flavor sterile solutions are disfavored at 95% C.L. by comparing global fit and SK d/n spectra

Oscillation analysis (flux constraint,sterile)

■ Allowed by SK zenith angle spectrum & flux at 95%C.L.

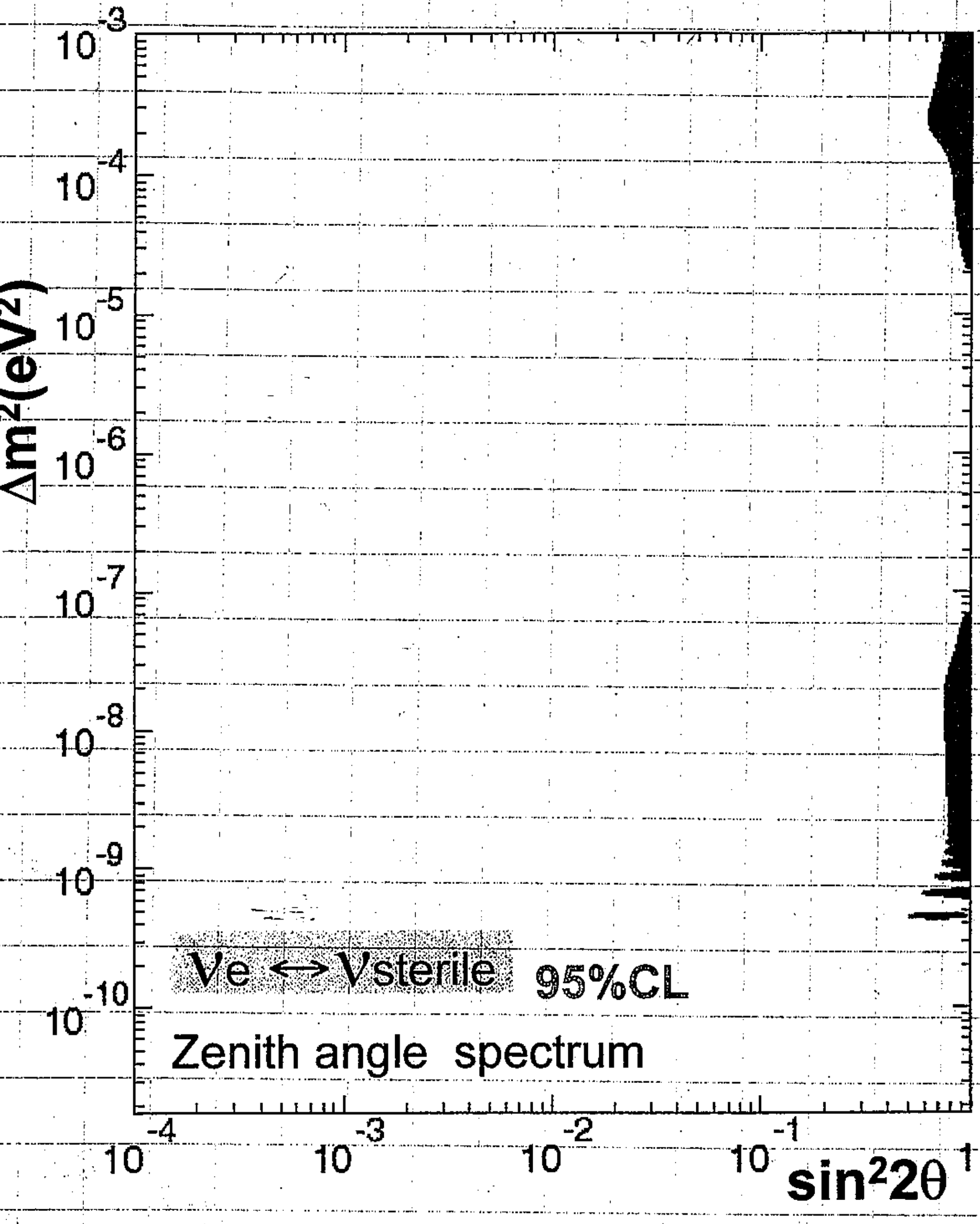

Large mixing is favored by SK d/n spectra with flux constraint (SK data only)

Hep neutrino

SSM$_{2000}$ prediction

^{8}B-neutrino $5.15 \times 10^6 (1.00 \pm ^{0.20}_{0.16})$ /cm^2/s
E_{max} = 15 MeV

Hep-neutrino 9.3×10^3 /cm^2/s
(2.1×10^3 /cm^2/s in BP98)
E_{max} = 18.8 MeV (no error estimate)
($(S(0)_{hep} = 10.1 \times 10^{-20}$ keV·b)

SK spectrum (1MeV binning upto 21 MeV)

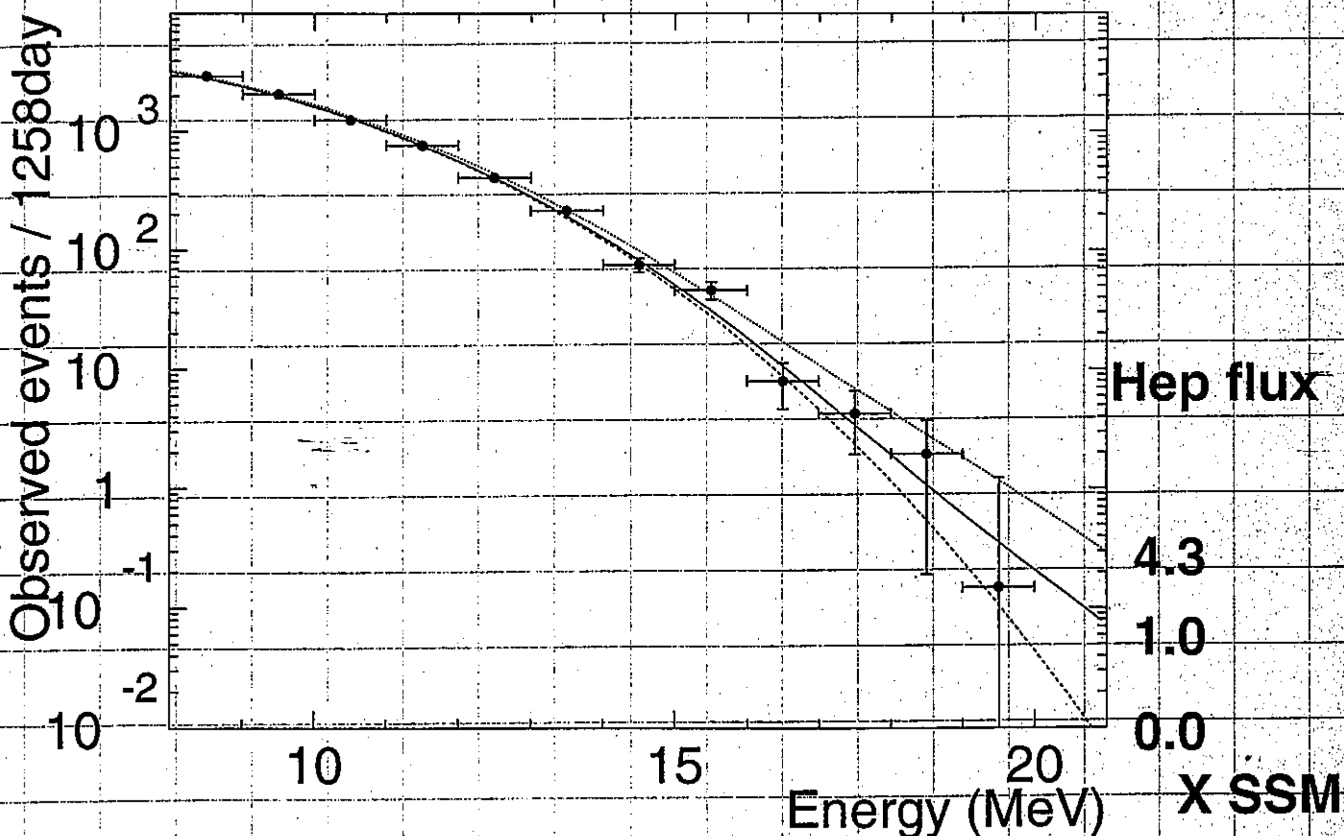

hep flux limit obtained using 18-21 MeV events

hep flux $< 40 \times 10^3$ /cm^2/sec

($<4.3 \times SSM_{BP2000}$)

SK detector maintenance

July – December, 2001

replace dead PMTs

What to do in future for solar neutrinos

Reduce background in lower E region

$\cos\theta_{sun}$ in low E region

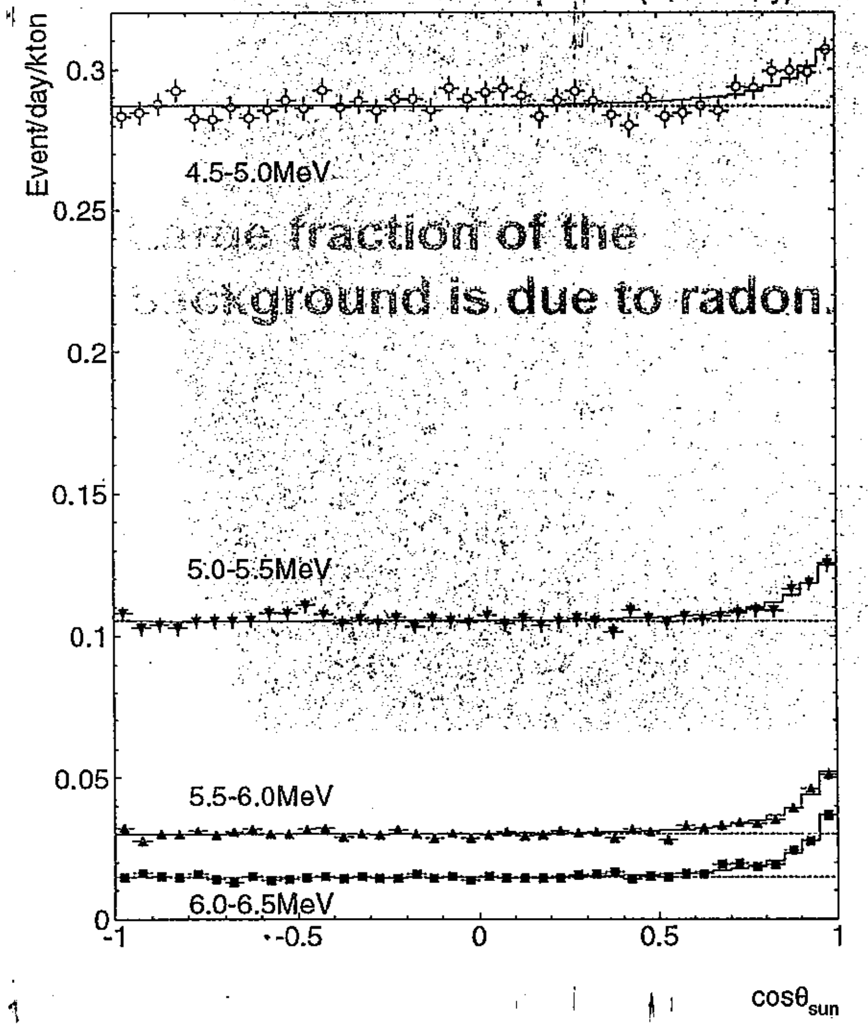

Vertex position distibution

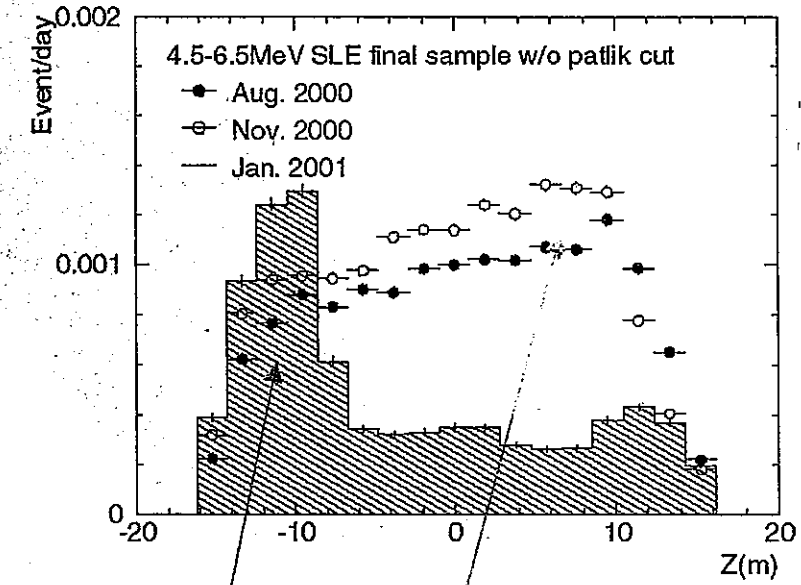

Source of radon is detector materials (PMT retc.).
Distributed over the detector by convection.

Water flow change for radon reduction

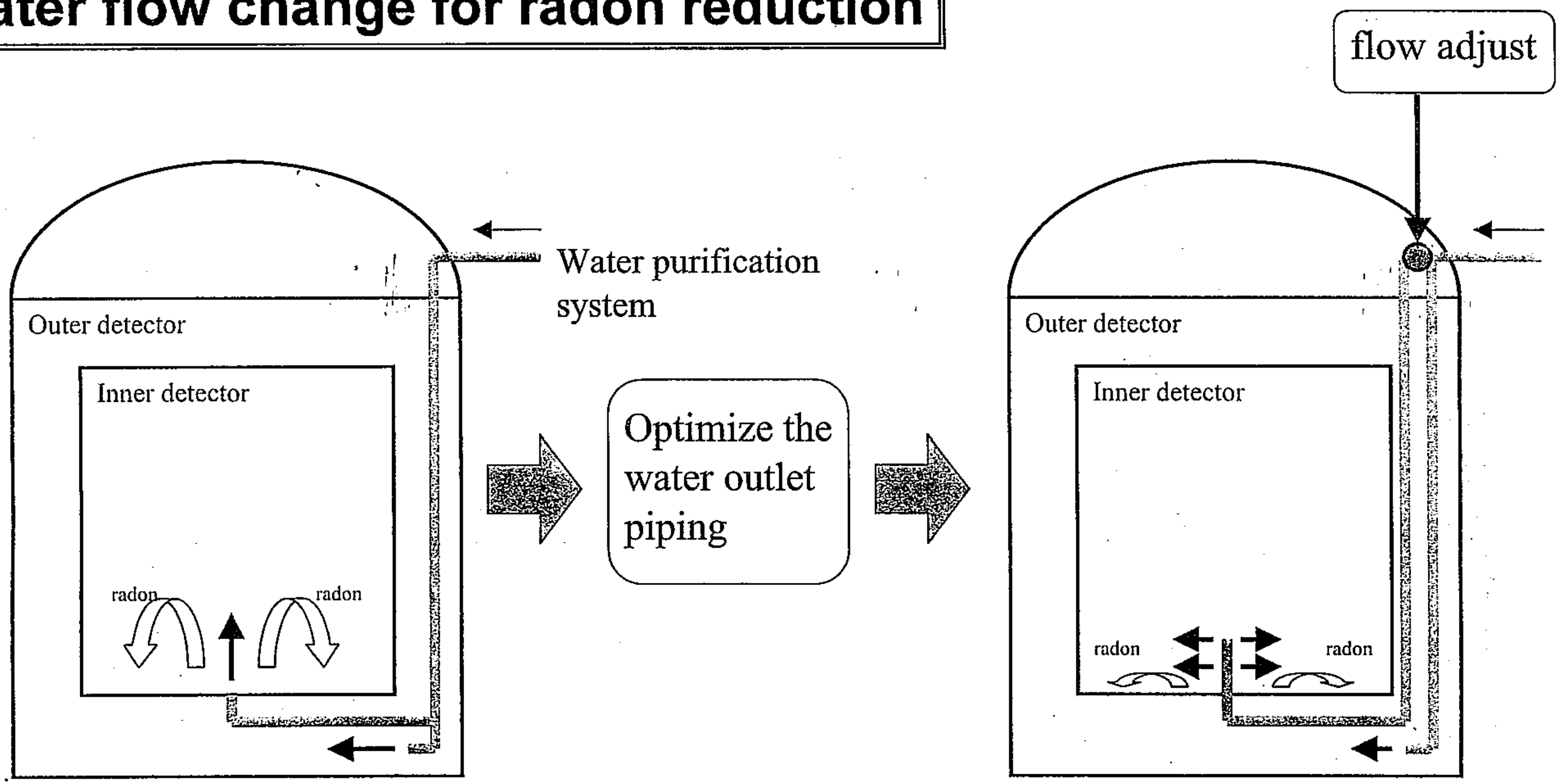

Now

- radon distributed in supplied water.
- Only single flow to the detector.

Future

- Reduce the water convection.
- Adjust water flow to inner and outer detectors.

Conclusions

- Precise measurement of $^{8}B\ \nu$ by SK was presented.
- Observed flux of is 45.1% of SSM_{BP2000} with 1% stat. and 3% syst. errors.
- Energy spectrum is consistent with flat.
- day/night difference is 3.3 ± 2.2 +1.3/-1.2 %.
- SMA and Just-so solutions in the global flux analysis are disfavored with 93 % C.L. by SK zenith-spectrum analysis for $\nu_e \rightarrow \nu_\mu (\nu_\tau)$ oscillations.
- Large mixing regions are favored with flux constraint.
- $\nu_e \rightarrow \nu_{sterile}$ solutions are disfavored with 95% C.L. by zenith-spectrum.
- Future radon background reduction is expected.